INHIBITORS OF BRUTON'S TYROSINE KINASE ALTER MACROPHAGE INFLAMMATION

INHIBITORS OF BRUTON'S TYROSINE KINASE ALTER NF-κB AND NLRP3 INFLAMMATION IN MACROPHAGES

By Darryl Yin-Lai Chan, BSc.

A Thesis Submitted to the School of Graduate Studies in Partial Fulfillment of the Requirements for the Degree of Master of Science

McMaster University MASTER OF SCIENCE (2022) Hamilton, Ontario

(Biochemistry)

TITLE: Inhibitors of Bruton’s tyrosine kinase alter NF-κB and NLRP3 inflammation

AUTHOR: Darryl Yin-Lai Chan, BSc (McMaster University)

SUPERVISOR: Dr. Jonathan Schertzer

NUMBER OF PAGES: xii, 80

LAY ABSTRACT

Obesity overwhelms fat storage sites and causes inflammation, which can contribute to metabolic disease. An important part of this inflammation is the NOD-like receptor family pyrin domain-containing 3 (NLRP3) inflammasome. This sensor of stress detects danger signals and produces molecules involved in inflammation. However, overactivation of NLRP3 can cause inflammatory diseases. Blocking another protein, Bruton's tyrosine kinase (BTK), can limit the activation of NLRP3 inflammasome. Our findings show that blocking BTK using drug inhibitors lowers inflammation caused by the NLRP3 inflammasome. Interestingly, we found that these drugs can lower inflammation without working on BTK, the protein that these drugs are designed to block. Understanding how these drugs are anti-inflammatory will help us understand the NLRP3 inflammasome, and how to lower inflammation during obesity and metabolic disease.

ABSTRACT

Obesity-related inflammation increases one's risk of developing cardiovascular disease, type 2 diabetes, among many other disorders. Energy imbalance during obesity overwhelms the adipose tissue leading to immune cell infiltration, elevations in pro-inflammatory cytokines, and consequent local and systemic insulin resistance. Certain potent pro-inflammatory cytokines are produced by the NOD-like receptor family pyrin domain-containing 3 (NLRP3) inflammasome. This metabolic danger sensor is involved in a variety of autoimmune and inflammatory conditions, hence regulation of this node as a therapeutic approach is a topic of great interest. To date, there is no clinically approved inhibitor of the inflammasome, which makes indirect targeting through endogenous molecules an attractive area of research. Bruton's tyrosine kinase has been shown to physically interact with NLRP3 inflammasome components and is required for its production of pro-inflammatory cytokine, IL-1β. However, the consequences of BTK inhibition on metabolic tissues like adipose tissue remain largely unstudied. *In vitro* experiments showed that pharmacological BTK inhibitors lower NLRP3 inflammasome priming and activation in macrophages. Bone marrow-derived macrophages (BMDMs) from a *Btk*-null mice strain treated with BTK inhibitors demonstrated lowering of lipopolysaccharide (LPS) -induced elevations in inflammatory cytokines. This effect was interestingly observed in both BMDMs derived from wild-type and *Btk*-null mice, postulating the idea that pharmacological inhibitors of BTK have anti-inflammatory properties that do not require the presence of the BTK gene product. Further, the optimized conditions for testing the influence of BTK inhibitors on adipose tissue insulin signaling *ex vivo* is outlined. Future work should focus on pinpointing off-

targets shared between BTK inhibitors to identify the node responsible for the observed anti-inflammatory effects. This research may lead to the development of an alternative therapeutic approach to treating inflammatory and autoimmune diseases mediated by the NLRP3 inflammasome.

ACKNOWLEDGEMENTS

I would like to thank my supervisor Dr. Jonathan Schertzer for giving me the opportunity to contribute to the amazing research efforts in his lab. Your scientific vigor, personable demeanor, and genuine compassion has not only inspired me as a researcher but as a person as well. It was your continual guidance, patience, and encouragement that made it possible for me to seamlessly progress through graduate school during a global pandemic. Although we did not have many opportunities to interact in-person during my first year, you made every effort to ensure that my graduate experience was supported even from afar, and for that I am extremely grateful. It was an absolute pleasure to be able to call myself a member of the Schertzer lab family.

Next, I would like to thank my mentor Dr. Nicole Barra for being the most understanding and compassionate teacher I could have asked for. You are the only person that can make the workload of doing research as a post-doctorate fellow, handling day-to-day lab business, and being an amazing mother, look effortless. Thanks to your mentorship, I was able to quickly learn the necessary lab techniques and start to perform experiments on my own. I wish you all the best as you welcome the newest member to the Barra family.

I would like to extend my gratitude to my colleagues of the Schertzer lab: Dr. Fernando Anhê, Dr. Brittany Duggan, Michael Huang, Anita Singh, Dr. Gabriel Anhê, Arshpreet Bhatwa, Nazli Robin, Danny Marko, May Nguyen, Dr. Hannah Fang, and Dr. Rodrigo Lacerda. I truly appreciate all the support and guidance I received for experiments and personal matters. You all made my graduate experience a very enjoyable one.

I would also like to thank my supervisory committee Dr. Geoff Werstuck and Dr. Sandeep Raha for your wisdom and advice on helping me thrive as a master's candidate. Your input greatly accelerated my research progression.

Last but not least, I would like to thank my family and friends for your unconditional love and support. In times of stress, it was your continued encouragement that helped me carry on. For that, I am forever grateful.

TABLE OF CONTENTS

LIST OF FIGURES

LIST OF TABLES

LIST OF ABBREVIATIONS

ANOVA	Analysis of variance
ASC	Apoptosis-associated speck-like protein containing a CARD
ATP	Adenosine triphosphate
BCR	B cell receptor
BMDM	Bone marrow derived macrophages
BTK	Bruton's tyrosine kinase
cDNA	Complementary deoxynucleic acid
CLL	Chronic lymphocytic leukemia
DAMP	Danger-associated molecular patterns
DMEM	Dulbecco's modified eagle medium
ELISA	Enzyme-linked immunosorbent assay
FBS	Fetal bovine serum
FFA	Free fatty acid
HbA1c	Hemoglobin A1c
HEK	Human embryonic kidney
IL-18	Interleukin-18
IL-1β	Interleukin-1 beta

IL-6	Interleukin-6
LPS	Lipopolysaccharide
MAPK	Mitogen-associated protein kinase
MCL	Mantle cell lymphoma
mTOR	Mammalian target of rapamycin
NF-κB	Nuclear factor kappa B
NLR	NOD-like receptor
NLRP3	NOD-like receptor family, pyrin domain-containing 3
NOD1	Nucleotide-binding oligomerization domain-containing protein 1
P/S	Penicillin/streptomycin
PAMP	Pathogen-associated molecular patterns
PBS	Phosphate buffered saline
RNA	Ribonucleic acid
ROS	Reactive oxygen species
RT-PCR	Real time polymerase chain reaction
SEM	Standard error of the mean
T2D	Type 2 diabetes
TLR	Toll-like receptors
TNF-α	Tumour necrosis factor alpha
XLA	X-linked agammaglobulinemia

DECLARATION OF ACADEMIC ACHIEVEMENT

The following is a declaration that the content of the research presented in this thesis has been completed by Darryl Yin-Lai Chan. The research study was designed by Dr. Jonathan Schertzer, who also contributed to the review and completion of this thesis. To the best of my knowledge, the content of this thesis does not infringe on the copyright of any others.

1.0 INTRODUCTION

1.1 Type 2 Diabetes

Diabetes is a chronic metabolic disease characterized by elevated blood glucose and impaired blood glucose control. As of 2019, global diabetes prevalence is estimated at over 463 million people (9.3% of global population).[1] The International Diabetes Foundation predicts that this number will increase by an additional 100 million within the next decade. Of the three main types, type 2 diabetes (T2D) accounts for 90% of all cases, the remainder being spread between type 1 or gestational diabetes.[2] Individuals with glycated haemoglobin A1c (HbA1c) levels above 6.5%, or fasting blood glucose levels above 125 mg/dL meet the diagnosis criteria for diabetes.[2]

T2D is caused by a progressive impairment of insulin production from the pancreatic β-cells relative to insulin action on target cells.[2] A decreased sensitivity to insulin, or insulin resistance, generally precedes overt T2D. Early in T2D progression, insulin resistance often coincides with a compensatory increase in the production of insulin. Higher levels of insulin can initially help control blood glucose, but persistent hyperinsulinemia can also exacerbate insulin resistance and promote obesity, thereby driving key factors in the progression from prediabetes to overt T2D.[2]

1.2 Obesity and Adipose Tissue Dysfunction

Obesity is a global concern of increasing proportions and now considered one of the largest contributors to poor health worldwide.[3] Following the current trajectory of obesity prevalence, approximately half of the global population will be classified as overweight by year 2030.[3] The clinical criteria for obesity is a body mass index (BMI) of 30 kg/m^2 or

higher.[4] Obesity is associated with an increased risk of numerous chronic co-morbidities including T2D, cancers, cardiovascular disease, and premature death.[5]

Obesity is characterized by maladaptive adipose tissue function and homeostasis.[2] Adipose tissue is a key site of energy storage, where lipids are stored as triglycerides in adipocytes.[6] Obesity generally results when there is an imbalance between the intake and expenditure of energy.[7] During obesity, the ability of adipocytes to store lipids can be overwhelmed and this nutrient overload in adipocytes can promote lipid spillover and result in ectopic lipid deposition in muscle and liver, contributing to local and systemic insulin resistance.[6]

Beyond its key role in metabolism, adipose tissue acts as both an endocrine and immunological organ. It has been shown that adipose tissue can secrete a variety of molecules including adipokines, cytokines, and chemokines.[8] Adipocytes and tissue-resident immune cells in adipose tissues can generate pro-inflammatory mediators. For example, elevated tumour necrosis factor-alpha (TNF-α), interleukin-6, and monocyte chemoattractant protein-1 (MCP-1) can promote a chronic inflammatory environment in adipose tissue during obesity, which can contribute to the development of insulin resistance and progression of T2D.[8,9]

Obesity-related inflammation also involves increased infiltration, expansion and pro-inflammatory polarization of immune cells, such as macrophages, into adipose tissue.[10] Once the contribution of immune cells to metabolic dysfunction in adipose tissue was realized, many connections between nutrients, metabolites, and immune function were discovered. For example, an elevation in free fatty acids (FFA) associated with obesity can program cellular metabolism to synergize with immunological ligands of innate

immune receptors such as toll-like receptors.[11] Innate immune ligands can work together to synergistically promote the activation of inflammatory pathways in a subset of adipose tissue resident immune cells.[12] FFAs can promote the polarization of these adipose tissue-resident macrophages towards a pro-inflammatory (M1) phenotype, which generates an inflammatory environment that impedes insulin signaling in adipocytes and contributes to insulin resistance.[10]

1.3 Innate Immunity

Obesity-related inflammation can disrupt key nodes in insulin signaling, leading to impaired insulin action in certain cell types.[13] Therefore, it is important to understand the immune components that propagate insulin resistance and progression of T2D.[9] Obesity is a key factor that promotes insulin resistance. Obesity is associated with compartmentalized changes in immune responses, including increased pro-inflammatory tone in adipose tissue.[14] In response to systemic insulin resistance, a compensatory increase in blood insulin can help maintain blood glucose control.[15] However, sustained elevation in insulin level can engage immune responses, thereby further promoting inflammation and insulin resistance.[16]

Inflammation acts as a first line of defense against danger signals like infection or tissue injury.[17] The innate immune system entrusts pattern-recognition receptors (PRRs) to detect components of foreign pathogens and damaged cells in order to elicit a protective response.[18] PRRs include toll-like receptors (TLRs), nucleotide-binding oligomerization domain (NOD)-like receptors (NLRs), among several other classes of innate immune proteins. PRRs recognize microbial-derived pathogen-associated molecular patterns (PAMPs) and host-derived signals of stress or damage known as

damage-associated molecular patterns (DAMPs). Notably, plasma membrane-residing TLRs, such as TLR4, detect circulating damage signals such as lipopolysaccharide (LPS), among other foreign or damaged cellular components.[19] Among NLRs, NLR family pyrin domain-containing 3 (NLRP3) also detects bacterial components, microbial and host DNA, as well as DAMPs such as high levels of ATP, uric acid, and cell stress induced by pore forming toxins.[17] NLRP3 has been described as a metabolic damage sensor because of the many metabolic stress or damage cues that this protein recognizes. The detection of these pathogen and/or damage signals induce the formation of large cytosolic protein complexes, called inflammasomes, which transduce inflammatory responses. PRR activation leads to downstream signaling which mounts a host cellular response in an attempt to eliminate the stressors. This mechanism involves multiple innate immune cells and can generate inflammatory signals such as elevated pro-inflammatory cytokines and reactive oxygen species (ROS) production. Macrophages are one key cell type that produce these early inflammatory signals to inform the host about infections, and to delay microbial expansion to allow time for an adaptive immune response to be engaged.[17]

However, immune responses can promote metabolic dysfunction where chronic low-level inflammation is sustained.[10] Upon PRR activation, the nuclear factor κB (NFκB) and mitogen-activated protein kinase (MAPK) pathways are engaged to initiate an inflammatory response. NF-κB-mediated cytokine and chemokines production, immune cell infiltration into adipose tissue, and stress kinase activation can cooperate to impair insulin signaling and contribute to insulin resistance.[20]

1.4 NLRP3 Inflammasome

1.4.1 Mechanism of Activation

NLR family pyrin domain-containing 3 (NLRP3) inflammasome is a multi-protein complex which acts as a metabolic danger sensor.[21] This inflammasome responds to a variety of danger signals such as pore forming toxins, cholesterol crystals, high levels of ATP, and xenobiotics.[22] The inflammasome complex consists of the sensor NLRP3, an adaptor apoptosis-associated speck-like protein containing a CARD (ASC), and pro-caspase-1.[23] The NLRP3 protein contains a C-terminal leucine-rich repeat domain (LRR), a central nucleotide-binding and oligomerization domain (NOD), and an N-terminal pyrin domain (PYD).[24] ASC contains a caspase-recruitment domain (CARD) and also a PYD domain, which mediates intra-complex interactions between NLRP3 and the recruited caspase-1.[22] The activation of NLRP3 inflammasome requires two steps: (1) a priming step, in which the NF-κB-mediated transcription of inflammasome components (such as NLRP3) and inflammasome effectors (such as pro-IL-1β) are up-regulated, and (2) an activation step, in which the oligomerized inflammasome complex generates active caspase-1, which can cleave specific cytokines such as IL-1β and IL-18 into their bioactive forms (Figure 1).[21]

1.4.2 Priming of the NLRP3 Inflammasome

The priming step of the NLRP3 inflammasome involves the engagement of any PRR or cellular response that activates NF-κB to increase transcription of inflammasome components, such as transcript levels of pro-IL-1β, pro-IL-18 and NLRP3. Then, the activation step involves NLRP3 inflammasome assembly which allows caspase-1 to auto-activate and cleave only certain cytokines such as pro-IL-1β and pro-IL-18 into

their active forms, which are then secreted into the cytosol.[24] Caspase-1 can cleave many proteins beyond IL-1β and IL-18, including components of glycolysis.[25,26]

1.4.3 Activation of the NLRP3 inflammasome

The NLRP3 inflammasome can be activated by numerous triggers including, but not limited to, pro-inflammatory lipids, changes in ion flux, purinergic receptor activation by extracellular ATP, membrane pore formation by nigericin, endoplasmic reticulum (ER) stress, and damage-induced release of mitochondrial reactive oxygen species (mtROS) and DNA (mtDNA).[27–31] NLRP3 inflammasome activity has been implicated in a range of inflammatory diseases, including atherosclerosis and T2D. The pro-inflammatory IL-1β and IL-18 have been linked to adipose tissue dysfunction and insulin resistance in mice models.[32]

Recent work in our lab has also identified statins, a class of cholesterol-lowering drugs as an activator of the NLRP3 inflammasome.[33,34]. In the presence of a priming agent like LPS, statins induce insulin resistance in adipose tissue via inflammasome-mediated production of IL-1β.[34] It was discovered that this pleotropic effect of statins on adipose tissue insulin resistance was propagated by lowering of protein prenylation. Statin-mediated adipose tissue insulin resistance also required signaling via the mitogen-activated protein kinase p38 and metabolic sensor mammalian target of rapamycin (mTOR) complex 1.[35] Despite these intriguing findings, not much is known about how statins generate the cellular activation signal and the direct link between statins and the inflammasome in adipose tissue.

The exact mechanism of the NLRP3 inflammasome activation under various stressors remains unclear. Nevertheless, the NLRP3 inflammasome plays an integral

role in the innate immune response and the development of insulin resistance and thus warrants research into understanding the role of activators and effectors of the inflammasome.[10]

1.4.4 NLRP3 inflammasome in metabolic disease

The NLRP3 inflammasome and IL-1β are inherently protective mediators of cellular homeostasis as it detects and responds to danger signals. However, unregulated activation of the inflammasome can contribute to a chronic inflammatory state. Several autoimmune conditions such as rheumatoid arthritis and systemic lupus erythematosus can be attributed to dysregulation of inflammasome activity.[36] Activation of the NLRP3 inflammasome signaling is implicated in graft-versus-host disease, Alzheimer's, obesity-induced asthma, and insulin resistance.[37–40] Pharmacological inhibition or genetic deletion of NLRP3 can mitigate high-fat diet-induced insulin resistance, dysglycemia, and β-cell dysfunction.[40–42] In the context of obesity-induced inflammation, an increase in caspase-1 activity coincides with adipocyte insulin resistance in response to high-fat diet feeding in mice.[43] Deletion of NLRP3 or caspase-1 in mice protects adipocytes from inflammation-induced insulin resistance.[43] These findings demonstrate a regulatory role of the caspase-1-containing NLRP3 inflammasome in adipose tissue inflammation and metabolism during obesity and insulin resistance.

1.4.5 Targeting the NLRP3 Inflammasome

It has been well-established that NLRP3 activation contributes to a chronic state of inflammation. This idea enticed much research into the regulation of NLRP3 inflammasome as a therapeutic approach to addressing these conditions. However,

inhibiting isolated components of the inflammasome comes with many potentially deleterious consequences. For example, blocking common inflammasome components such as ASC, may result in risk of immune suppression and increase susceptibility to infections.[44] Therefore, blocking downstream effectors, such as IL-1 receptor or IL-1β has been proposed as an alternative. IL-1β is implicated as the driver of many NLRP3-mediated disorders, and has been a prime target for altering the effector function of the NLRP3 inflammasome.[45] In fact, there are three IL-1 inhibiting proteins that are clinically approved for the therapeutic purposes. Anakinra (a modified IL-1 receptor antagonist), canakinumab (a monoclonal antibody against IL-1β), and rilonacept (a soluble pseudo-receptor specific to IL-1α and IL-1β) have all shown promise in the treatment of certain NLRP3-mediated diseases, like atherosclerosis, arthritis, and gout.[46–49] However, the challenge with this therapeutic approach is its lack of selectivity at the key site of inflammation and redundancy in immune effectors. IL-1β is only one pro-inflammatory effector and obesity increases many inflammatory effectors controlled by the NLRP3 inflammasome, including IL-18 and other targets of caspase-1.

The progress of NLRP3 inhibitor development has largely been hindered by the incomplete understanding of the central activation mechanism. This lapse in knowledge means that any efficacious response elicited by these compounds may be a result of indirectly targeting a related pathway. Currently, compound CP-456,773 (also known as CRID3 and MCC950) is the most studied NLRP3 inhibitor. This compound binds the NACHT domain and stabilizes the inactive conformation of NLRP3.[50] This action potently inhibits ATP-induced, NLRP3-mediated IL-1β production, with a half-maximal inhibitory concentration (IC_{50}) of 8.1 nM in human monocytes.[51] It is currently the most

promising inhibitor of NLRP3 due to the low dose required for inhibition and less off-target toxicities relative to other inhibitors.[44] Nevertheless, more research needs to be done in order to solidify the efficacy and specificity of this compound to target NLRP3. This compound did enter phase II clinical trials by Pfizer for rheumatoid arthritis, however, was discontinued due to an increase risk of liver toxicity.[44] Overall, more rigorous research efforts must target uncovering the mechanism of action of these NLRP3 regulatory compounds. To date, there remains to be no clinically approved inhibitors for direct targeting of NLRP3.

1.5 Bruton's tyrosine kinase

Bruton's tyrosine kinase (BTK) was initially discovered as the genetic cause of X-linked agammaglobulinemia (XLA), which is a mediator in B cell receptor (BCR) signaling.[52,53] BTK is crucial for the proliferation, differentiation, and survival of leukemic cells in many B cell malignancies, which makes it a prime treatment target.[54] It is important to note that BTK is also expressed in myeloid cells like macrophages, neutrophils, mast cells, and dendritic cells.[23] BTK contains a N-terminal pleckstrin homology (PH) domain capable of binding to phosphatidylinositol (3,4,5)-trisphosphate (PIP_3), a proline-rich Tec homology domain, and Src homology (SH) 2 and 3 domains.[53] The catalytic activity of BTK has links to at least three major signaling pathways, namely phospholipase C, phosphoinositide-3-kinase/Akt, and NF-κB.[53] The multi-faceted nature of BTK also includes roles in microbial sensing via several toll-like receptors, Fc and growth factor receptor signaling, phagocytosis, platelet activation, and immune cell differentiation in neutrophils and B cells.[55]

In the last decade, several studies have presented BTK as a regulator of NLRP3 inflammasome action. It was demonstrated that BTK is required for inflammasome-mediated IL-1β release from murine macrophages.[23,56] Upon NLRP3 activation, BTK is rapidly phosphorylated, and BTK physically interacts with inflammasome components NLRP3 and ASC.[23] This interaction induces the oligomerization of ASC and the subsequent activation of caspase-1. XLA patient-derived peripheral blood mononuclear cells (PBMC) had reduced inflammasome activity, further suggesting that BTK is intimately involved in regulating NLRP3 inflammasome activation.[23]

1.5.1 Inhibition of Bruton's tyrosine kinase

The irreversible BTK inhibitor, ibrutinib (PCI-32765) has shown promise in treating patients with relapsed/refractory chronic lymphocytic leukemia (CLL) and mantle-cell lymphoma (MCL). Due to its efficacy, ibrutinib was approved as the initial treatment option for patients with CLL in 2016.[57] BTK was originally studied in the context of oncology and immune receptor signaling, however, later studies investigating the deficiency and inhibition of BTK demonstrated its potential involvement in inflammatory disorders, such as autoimmune arthritis, ischemic brain injury, and colitis.[58–60]

Ibrutinib is designed to bind Cysteine-481 on BTK, however, off-target binding of several other homologous cysteine-containing kinases lead to side-effects.[61] These off-target toxicities include bleeding, impaired platelet activation and aggregation.[62,63] Despite its clinical efficacy, the reported off-target effects fostered the need for an alternative inhibitor with a higher selectivity for BTK. Acalabrutinib (ACP-196) was designed as a more selective BTK inhibitor with the goal of achieving similar therapeutic outcomes, while minimizing off-target effects associated with ibrutinib use.[64] Although

acalabrutinib has a higher half maximal inhibitor concentration (IC_{50}) value than ibrutinib (5.1 vs 1.5 nM, respectively), acalabrutinib is a more selective inhibitor with lower IC_{50} against other cysteine-containing kinases with Cys-481 that aligns with BTK.[64]

Liu et al. in 2017 proposed that BTK could act as a point of regulation for NLRP3-associated inflammation.[23] They observed significant NLRP3 inflammasome loss-of-function in both BTK-deficient cells from human and mice models, as well as pharmacological inhibition of BTK *in vivo*. These authors also demonstrated that BTK inhibition effectively impaired IL-1β processing and release in human primary macrophages. These data highlighted the potential of targeting NLRP3 inflammasome-related inflammatory disorders through BTK.[23]

A recent study involving an *in vitro* model of tumour-associated macrophages (TAMs) demonstrated the efficacy of ibrutinib at inhibiting BTK phosphorylation and significantly impaired the ability of these TAMs to produce IL-1β.[65] These findings further support the potential for the clinical use of ibrutinib in lowering inflammation-related disease progression. It is intriguing to speculate that inhibiting BTK with clinically approved drugs could lower NLRP3 inflammasome activation in obesity or with statin treatment in people at risk of T2D. Therefore, mechanistic work understanding the interaction of BTK inhibitors and NLRP3-mediated inflammation is warranted.

Purvis et al. in 2020 showed that BTK expression and activation are increased in wild-type mice fed a high-fat diet (HFD).[66] These authors also showed that inhibition of BTK in HFD-fed mice decreases macrophage NF-κB and NLRP3 inflammasome activity in the liver and kidney. They showed that chronic treatment of the BTK inhibitor, ibrutinib (3 or 30 mg/kg by oral gavage 5 days per weeks for 6 weeks) reduced metabolic

inflammation in the liver and adipose tissue, which consequently resulted in improved glycemic control and insulin sensitivity in the liver.[66] These highlight the potential for ibrutinib and other BTK inhibitors to lower inflammation in metabolic disease.

A recent paper by Bittner and colleagues provided exciting insight into the mechanistic link between BTK and NLRP3 inflammasome activity.[67] These authors defined four tyrosine residues along the polybasic linker (PBR) between the NLRP3 pyrin domain (PYD) and NACHT domain, where BTK directly alters these specific residues to alter the overall charge of the PBR peptide sequence. They also found that BTK's regulatory actions include subcellular localization of NLRP3, oligomerization and interaction with inflammasome components (NLRP3-ASC contact), ultimately leading to modulation of IL-1β release.[67] These findings therefore suggests that BTK activation directly leads to activation of the NLRP3 inflammasome, and by extension, inhibition of BTK impedes the ability of the NLRP3 inflammasome to produce IL-1β. This discovery places BTK as a target in the regulation of NLRP3 inflammasome-mediated processes relevant to obesity and insulin resistance, but little is known in adipose tissue.

1.5.2 Shortcomings

Since idea of targeting BTK as a regulator of NLRP3 inflammasome surfaced nearly a decade ago, there has been exhaustive efforts into determining the efficacy of BTK inhibition on NLRP3-mediated diseases. Studies have found potential for BTK inhibition on acute (e.g., ischemic stroke, graft-versus-host disease, COVID-19) and chronic NLRP3-mediated diseases (e.g., neurodegeneration, atherosclerosis, metabolic inflammation). Despite this, it remains a fact that little is known about the differential effect of inhibiting BTK function in B cells versus in macrophages. This question needs

to be addressed perhaps with more targeted delivery of drug inhibitors, or cell-type-specific knockout of *Btk*. Until the distinction between cell type specific BTK functions is clarified, it would appear BTK inhibition remains more suitable for use in acute conditions rather than chronic diseases. Moreover, the interaction between BTK and NLRP3 in macrophages has been investigated. However, future research should explore other cell types such as neutrophils, Kupffer cells, hepatocytes and adipocytes.

2.0 RATIONALE, HYPOTHESIS, RESEARCH AIMS

2.1 Rationale

BTK has been implicated as a regulator of NLRP3 inflammasome activity.[23,56,66] The physical interaction between BTK and inflammasome components has been well-established.[66,67] Despite these connections, much remains unclear regarding the efficacy of BTK inhibition on metabolic tissue inflammation downstream of the NLRP3 inflammasome. Specifically, effect of BTK inhibition on tissue-localized insulin resistance remains to be explored. This knowledge gap, along with the ever-increasing promise of BTK as a regulator of inflammasome function, inspired our assessment of Ibrutinib and Acalabrutinib in NLRP3-mediated inflammation in macrophages and metabolic inflammation and insulin resistance in adipose tissue.

2.2 Hypothesis

We hypothesize that pharmacological BTK inhibitors reduce inflammation and insulin resistance in macrophages by lowering activation of the NLRP3 inflammasome.

2.3 Research Aims

1) Determine if pharmacological BTK inhibitor treatment alter priming and/or activation of the NLRP3 inflammasome in murine macrophages
2) Assess the difference between *Btk*-deficient and BTK inhibitor-treated murine macrophages in the context of NLRP3 inflammasome priming and activation
3) Determine the effect of BTK inhibition on murine adipose tissue insulin resistance induced by activators of the NLRP3 inflammasome

3.0 EXPERIMENTAL METHODOLOGY

3.1 Mice

Wild-type (WT) C57BL/6J, NLRP3$^{-/-}$, CBA/CaJ, and mutant CBA/CaHN-Btk^{xid} mice were used for bone marrow harvests and adipose tissue extractions. C57BL6/J were originally from The Jackson Laboratory and bred in-house. NLRP3$^{-/-}$ mice (>10 generations backcrossed to C57BL/6J) were from Professor Nicolas Fasel (Université de Lausanne, Lausanne, Switzerland) and were originally provided by Dr. Dana Philpott (University of Toronto, Toronto, ON, Canada). The two CBA-background strains were from The Jackson Laboratory (#000654, #001011, respectively).

3.2 Reagents and Antibodies

For a full list of reagents and antibodies used in experiments, please refer to the details contained in Tables 1 and 2.

Table 1: Reagents used in the studies.

Reagent	Manufacturer	Reagent	Manufacturer
10X PCR Gold Buffer	Applied Biosystems	Homogenizer Ceramic Beads	Omni International
5X SSIV Buffer	Invitrogen	Ibrutinib	Tocris Bioscience
Acalabrutinib	Selleckchem	Isopropanol	VWR
Acrylamide (40%)	Fisher BioReagents	LPS-*E. coli*	Invivogen
AmpliTaq Gold	Applied Biosystems	Methanol	VWR
Ammonium Persulfate	Sigma	$MgCl_2$	Applied Biosystems
Anhydrous Ethanol	Fischer Scientific, Commercial Alcohol	Molecular Grade Water	Mediatech
Atorvastatin	Cayman Chemical	Nigericin	Invivogen
BSA	BioShop	Normocin	Invivogen
Chloroform	Anachemia	NovoRapid® Insulin	Novo Nordisk
Clarity Max™ Western ECL Substrate	Bio-Rad	Oligo-dt(18)	McMaster Mobix Lab
cOmplete Protease Inhibitor Cocktail Tablets	Roche	Oligonucleotide Primer	McMaster Mobix Lab
Dithiothreitol (DTT)	Invitrogen	PBS	Thermo Fisher

DMEM	Wisent Bio Product	Penicilin/streptomycin	Wisent Bio Product
DNAse I 10X Reaction Buffer	Invitrogen	Random Hexamers	McMaster Mobix Lab
DNAse I Amplification Grade	Invitrogen	Random Pentadecamers	McMaster Mobix Lab
dNTP (dATP, dTTP, dGTP, dCTP)	Wisent Bio Product	RiboZol™ RNA Extraction Reagent	VWR
EDTA	Sigma	Sodium Chloride	BioShop
Fetal Bovine Serum	Wisent Bio Product	Sodium Dodecyl Sulfate	Sigma
Gentle ReView™ Stripping Buffer	VWR	Sodium Fluoride	Sigma
GlutaMAX	Thermo Fisher	Sodium Pyrophosphate Decahydrate	Sigma
Glycine	BioShop	Sucrose	Sigma
HCl	Caledon	Tris	BioShop
HEK-Blue Detection	Invivogen	Triton™ X-100	Sigma
HEK-Blue Selection	Invivogen	Tween® 20	Sigma
HEPES	BioShop		

Table 2: Antibodies used in the studies.

Antibodies	Catalogue number	Manufacturer
IL-1β	DY401	R&D systems
IL-6	DY406	R&D systems
Phospho-Akt (Ser^{473})	#4058L	Cell Signaling
Akt	#9272S	Cell Signaling
Anti-rabbit IgG, HRP-linked	#7074S	Cell Signaling

3.3 Cell Culture

3.3.1 HEK-293T Cell Culture

Two commercially available embryonic kidney cell lines (HEK-Blue hTLR4 and hNOD1 cells; InvivoGen, San Diego, CA) were used for analysis of NF-κB activation. HEK-hTLR4 and HEK-hNOD1 cells were cultured in growth media (DMEM, 4.5 g/L glucose, 10% (v/v) FBS, 100 U/mL penicillin, 100 µg/mL streptomycin, 100µg/mL Normocin, 2 mM of L-glutamine) for one passage post-thaw. Thereafter, the cells

cultured to 70% confluency before passage in selection media (growth media supplemented with one sachet of 1X HEK-Blue Selection for hTLR4 cells or supplemented with 30 µg/mL of blasticidin and 100 µg/mL of zeocin for hNOD1 cells). HEK cells are resuspended in treatment-supplemented HEK-Blue Detection media and seeded onto 96-well plates (25,000 cells/well). The cells are incubated for 24 hours and then analyzed on a spectrophotometer at 630 nm absorbance.

3.3.2 Primary Mouse Macrophages

Bone marrow content was extracted from femur and tibia of C57BL/6J, CBA/CaJ, or CBA/CaHN-Btk^{xid} mice approximately 20-25 weeks of age. Bone marrow-derived macrophages (BMDMs) were cultured for 7-10 days in Dulbecco's Modification Eagle's Medium (DMEM) with L-glutamine and sodium pyruvate. The medium was supplemented with 1% penicillin and streptomycin, and 15% L929-conditioned media for differentiation. The BMDMs were washed with serum-free media and treated with atorvastatin (1 µmol/L) for 22 hours in DMEM and LPS (200 ng/mL) was added during the final 4 hours. Ibrutinib or acalabrutinib (various concentrations) was added during the statin treatment period.

3.3.3 Adipocytes

3T3-L1 pre-adipocytes (ATCC, Rockville, MD) were differentiated for 8-12 days. Pre-adipocytes were seeded in 12-well plates and allowed to grow to confluency in basal media (BM: DMEM, 10% FBS, 1x GlutaMax, 1x penicillin/streptomycin). At 48-72 hours post-confluency, media was changed to differentiation media 1 (DM I: BM, 0.5 mM 3-isobutyl-1-methylxanthine, 0.25 µM dexamethasone, 1 µg/mL insulin, 2 µM rosiglitazone) for 48 hours, followed by a media change to DM II (BM, 1 µg/mL insulin)

for two 48-hour periods. After this, media is changed back to BM and changed daily. Between day 8-12 post-confluency, cells are assessed for differentiation and used for experiments. 3T3-L1 adipocytes were pre-incubated with either ibrutinib (10 µM) or acalabrutinib (50 µM) for one hour before being exposed to FK-565 (10 µg/mL) for 48 hours. Cells were either left unstimulated or stimulated with 100 nM of insulin for the final 10 minutes before cells were lysed and prepared for immunoblotting. Each experimental replicate (n) represents an individually treated and quantified culture well containing 3T3-L1 adipocytes.

3.4 Adipose Tissue Explants

C57BL/6J, CBA/CaJ, and CBA/CaHN-Btk^{xid}/J mice that were between 20 and 45 weeks-old were euthanized by cervical dislocation and gonadal adipose tissue was extracted. The extracted tissue was minced into pieces of ~5 mg in DMEM with 10% FBS. After 1-2 hours of equilibration, 25 mg of explant tissues were placed in serum-free DMEM and treated with atorvastatin (1 µmol/L) for 22 hours and LPS (2 µg/mL) was added for the final 4 hours. At the end of treatment, these explants were stimulated with insulin (0.3 nmol/L) for 10 minutes, and immediately flash frozen. Frozen samples were added to SBJ lysis buffer and mechanically homogenized with ceramic beads. The lysis buffer used was composed of SBJ buffer (0.05M HEPES, 0.15M NaCl, 0.1M NaF, 0.01M Na pyrophosphate, 0.005M EDTA2H2O, 0.25M sucrose), 1% Triton-X, and cOmplete protease inhibitor cocktail tablet. Adipose tissue lysates were used for immunoblotting. Each experimental replicate (n) represents an individually treated and quantified culture well containing 5 pieces of tissue explants.

3.5 Immunoblotting

Protein was extracted from adipose tissue lysates by mechanical homogenization in lysis buffer cocktail as described above. Protein concentration was quantified using the Pierce BCA protein assay (Thermo Fisher Scientific). Samples were prepared with Laemmli sample buffer and resolved on 7.5% polyacrylamide gels. Samples were then transferred onto PVDF membranes using the Bio-Rad Trans-Blot® Turbo™ Transfer System. Membranes were blocked in 5% BSA solution, followed by an overnight incubation in primary antibody. Primary antibodies used included P-Akt (S473) rabbit mAb, Akt rabbit Ab. After this, the membranes were washed 4 x 15 minutes with TBS-Tween (TBS-T). Then membranes were incubated with secondary antibody for 1 hour, and then wash step is repeated. Membranes were incubated in Bio-Rad ClarityMax™ Western ECL Substrate for ~2 minutes before visualization and imaging on the Bio-Rad ChemiDoc™ MP Imaging System. Membranes were stripped of antibodies between different primary antibody probes using Gentle ReView™ Stripping Buffer (N552-1L, VWR) at 30°C for 27 minutes. Quantification of bands was performed using Bio-Rad Image Lab Software.

3.6 Gene Expression Analysis

3.6.1 RNA Extraction

Approximately 250,000 BMDMs were collected in 0.3 mL of TRIzol®. All samples were mixed well with 100 µL of chloroform and incubated for three minutes at room temperature. Samples were then centrifuged at 12,000 x g for 10 minutes at 4°C. The separated aqueous phase was then transferred into a fresh tube containing 150 µL of isopropanol to precipitate RNA. Samples were mixed well and incubated at room

temperature for at least 20 minutes before another round of centrifugation at 12,000 x g for 10 minutes at 4°C. Supernatant was decanted and RNA pellet was washed twice with 75% ethanol, with a 10-minute spin in between each wash. Following last wash, the tubes were left open to allow for the remaining ethanol to evaporate before the RNA pellet was dissolved in pre-heated Ultra-Pure water. Samples were incubated at 55°C for 15 minutes and RNA content was quantified by spectrophotometry. The RNA content of each sample was equalized to 50-250 ng/µL with Ultra-Pure water.

3.6.2 cDNA Synthesis

For each sample, 200-1000 ng of RNA was mixed with 0.5 µL of DNase I 10x reaction buffer and 0.5 µL of amplification grade DNase I for 15 minutes at room temperature. After which, 0.5 µL of EDTA (25 mM), 0.5 µL of dNTP (10 mM) and 0.5 µLof random hexamer primer (250 ng) were added to each sample. Samples were incubated in the SimpliAmp Thermal Cycler (Applied Biosystems) at 95°C for 10 minutes to inactivate DNase I and 55°C for 10 minutes to anneal cDNA synthesis primer. After this, 2 µL of 5x SuperScript™ IV buffer, 0.5 µL of DTT (0.1 M), 0.5 µL of Ultra-Pure water, and 0.5 µL of SuperScript™ IV enzyme was added to each sample. The samples were then incubated at 55°C for 10 minutes and 80°C for another 10 minutes. cDNA was diluted 1:10 in Ultra-Pure water.

3.6.3 RT-PCR Reactions

For real-time polymerase chain reaction (RT-PCR), 10 µL of cDNA samples were mixed with 10 µL of master mix (5.1 µL Ultra-Pure water, 2 µL 10x PCR gold buffer, 2 µL $MgCl_2$, 0.4 µL dNTP (10 mM), 0.1 µL AmpliTaq® Gold, 0.4 µL TaqMan primer). For full list of commercial TaqMan primers used, refer to Table 3. RT-PCR was performed using

Rotor-Gene Q (Qiagen), at 95°C for 10 seconds, then 58°C for 45 seconds, repeated for 40 cycles. All genes were normalized to housekeeping gene *Rplp0* as a control using the delta-delta Ct method.

Table 3: Primers used in RT-PCR

Primer	Gene	Catalogue Number	Manufacturer
Rplp0	Rplp0	Mm01974474_gH	Thermo Fisher
Il1β	Interleukin 1-beta	Mm00434228	Thermo Fisher
Nlrp3	NLR Family Pyrin Domain Containing 3	Mm00840904_m1	Thermo Fisher
Il6	Interleukin 6	Mm00446190	Thermo Fisher
Tnf	Tumour necrosis factor	Mm00441891	Thermo Fisher
Il10	Interleukin 10	Mm00439616	Thermo Fisher

3.7 Cytokine Release

Cell supernatants collected from 2.5 x 10^6 murine BMDMs were used to quantify secreted levels of IL-1β and IL-6 by enzyme-linked immunosorbent assays (ELISAs) according to the manufacturer's protocol. IL-1β (DY401) and IL-6 (DY406) -specific Duo-Sets were used (R&D Systems, Table 2).

3.8 Single Nucleotide Polymorphism Genotyping

3.8.1 DNA Extraction

CBA/CaJ and CBA/CaHN-Btk^{xid}/J mice were anesthetized by isoflurane. The mice tails were cleaned with ethanol, after which 0.5 cm of tail segment was cut off from the end. The cut wound was chemically cauterized using silver nitrate sticks. DNA was extracted from tail samples according to the manufacturer's protocol (Wisent).

3.8.2 End-point Analysis

100 ng of DNA sample were combined with 0.4 µM of Forward Primer (16120) and 0.4 µM of Reverse Primer (16121)… As well, the solution was mixed with 0.15 µM of wild-type probe and 0.15 µM of mutant probe. The wild-type probe carries a VIC fluorescent tag on its 5’ end, while the mutant probe carries a FAM fluorescent tag. Both probes have a QSY quencher at the 3’ end. This ensures that there will be no fluorescence unless the fluorescent tag and the quencher are physically separated. Presence of the transgene of interest causes the specific probes to bind, and separation of the fluorescent tag and quencher will result in fluorescent signal. This mix was diluted 1:1 with TaqMan Fast Advanced Mix (2x) and used for end-point analysis. The samples were run using the Rotor-Gene Q system (Qiagen). The system was run on a manually inputted temperature profile which consists of an initial 60°C hold for 30 seconds, followed by a “hot-start” 95°C hold for 5 minutes, then it enters a 40-cycle phase where each cycle reaches 95°C for 15 seconds then drops to 60°C for 90 seconds. Data is acquired during the 60°C portion of each cycle. Allelic discrimination analysis was determined using the Rotor-Gene Q software.

3.9 Statistical Analysis

Statistical significance determined by unpaired two-tailed t-test or analysis of variance (ANOVA) where appropriate. D’Agostino-Pearson test is used to determine normality by how much the dataset differs from a Gaussian distribution, considering factors such as skewness and kurtosis. Unpaired two-tailed t-tests were used to determine differences between two groups when the data were normally distributed. One-way ANOVA was used to determine differences among three or more groups for in

a normally distributed dataset. A Dunnett or Bonferroni test was used to correct for multiple comparisons. Two-way ANOVA was used to determine how two independent variables affect a response variable and whether an interaction exist between them. All results were expressed as mean ± standard error of the mean (SEM) with $p < 0.05$ considered significant. All data presentation and statistical analyses were performed using GraphPad Prism 8 Software.

4.0 RESULTS

4.1 Effect of BTK inhibition on TLR4- and NOD1-mediated activation of NF-κB

We examined the effect of BTK inhibition on NF-κB signaling, which is a transcription factor linking PRR stimulation and increased gene expression of inflammasome components and effectors genes such as *Il-1β*. NF-κB activation was induced by LPS treatment and quantified using the HEK-Blue™ hTLR4 Reporter System. A preliminary experiment was performed by treating HEK-293T cells with a range of LPS doses (0.25-500 ng/mL). From the results, we determined that the LPS dose of 100 ng/mL reliably produced a robust elevation in NF-κB activation, therefore this LPS dose was used to further test the effect of BTK inhibitor treatment (Supplementary Figure 1A). We then assess the effect that various doses of Ibrutinib (0.1-10 μM) and Acalabrutinib (1-50 μM) had on LPS-induced NF-κB activation. We found that ibrutinib at 5 and 10 μM, and acalabrutinib at 50 μM significantly reduced the LPS-induced action of NF-κB (Figure 3A, 3B).

We next determined if lower NF-κB activation after BTK inhibition is specific to TLR4-ligands or if this extends to ligands of other pattern recognition receptors. We used the HEK-Blue™ hNOD1 Reporter System and performed a similar experiment using FK-565, a synthetic NOD1 receptor ligand. Again, a preliminary experiment was performed to determine optimal dose of FK-565 for induction of NF-κB activation, where a range of doses (10-100 ng/mL) were tested. The results showed that NF-κB activation was most robust at 100 ng/mL (Supplementary Figure 1B). We then tested various doses of ibrutinib (0.1-10 μM) and acalabrutinib (1-50 μM) on FK-565 treated HEK-293T cells. We found that ibrutinib at doses above 1μM, and acalabrutinib at doses above 20

μM significantly reduced NF-κB activation induced by 100 ng/mL of FK-565 (Figure 3C, 3D). This result supports the concept that BTK inhibitors can lower NF-κB-mediated inflammation and that BTK is involved the priming step of the NLRP3 inflammasome in response to multiple microbial triggers of PRRs.

4.2 Transcript levels of inflammatory genes during LPS exposure in response to BTK inhibition

4.2.1 BTK inhibitors mitigate LPS-induced inflammatory gene expression in macrophages

Using LPS as an inflammasome priming signal, we then sought to determine the effect of BTK inhibitor treatment on inflammatory gene expression. We treated BMDMs harvested from C57BL/6J mice with various concentrations of ibrutinib (0.1-10 μM) or acalabrutinib (1-50 μM) for 22 hours and primed the cells with LPS (200 ng/mL) for the final 4 hours of treatment. The timing of LPS exposure is due to the finding that NF-κB-relevant genes exhibit a peak of expression 4 hours following LPS treatment.[68] We suspected that BTK inhibitors would require a relatively longer exposure time to confer its drug effect, so we set treatment duration at 22 hours to match with our previously optimized model of statin-induced inflammation.[34]

LPS treatment alone significantly increased transcript levels of inflammasome effector and component genes, *Il-1β* and *Nlrp3*, as well as inflammatory genes like *Il-6*, *Tnf*, *Il-10* (Figure 4A, 4B). The data showed that ibrutinib at doses above 5 μM and acalabrutinib at doses above 20 μM lowered the LPS-induced increase in *Il-1β* expression down to near-control levels (Figure 4A, 4B). While no significant differences were observed in the expression of *Nlrp3* and *Il-6* at all tested ibrutinib doses,

acalabrutinib at doses above 20 μM brought down the LPS-induced elevations in expression of *Nlrp3*, *Il-6*, *Tnf* and *Il-10* back to near control levels. (Figure 4B). This data shows that ibrutinib treatment only lowers LPS-induced upregulation of *Il-1β*, but not other inflammatory genes like *Il-6*. Meanwhile, acalabrutinib at a sufficiently high dose (>20 μM), can significantly reduce not only LPS-induced elevations in the inflammasome effector gene, but the expression of other inflammatory genes as well.

4.2.2 BTK inhibitor treatment reduces inflammatory gene expression in macrophages after NLRP3 inflammasome activation

Next, we wanted to determine if adding an inflammasome activator like atorvastatin, in the treatment along with LPS stimulation (200 ng/mL) would affect the ability of these BTK inhibitors to reduce the elevation in inflammatory gene expression. We treated BMDMs harvested from C57BL/6J mice with various doses of ibrutinib or acalabrutinib with 1 μM of atorvastatin for 22 hours, then added 200 ng/mL of LPS for the final 4 hours of treatment as an inflammasome priming signal. Here, we observed that LPS + atorvastatin alone increased transcript levels of all inflammatory genes (*Il-1β*, *Il-6*, *Tnf*) (Figure 5A, 5B). Ibrutinib treatment at all tested doses significantly reduced this LPS and atorvastatin induced elevation in expression levels of *Il-1β*, *Il-6*, and *Tnf* (Figure 5A). Further, we found that acalabrutinib at doses above 20 μM lowered the increase in expression of *Il-1β*, *Il-6*, and *Il-10* (Figure 5B). Interestingly, only ibrutinib (>0.1 μM), not acalabrutinib, was able to bring down LPS and atorvastatin induced increase in *Tnf* expression. Taken together, the BTK inhibitors, ibrutinib and acalabrutinib, lower the expression of inflammasome components and effectors in BMDMs in the presence or absence of NLRP3 activator such as a statin.

4.2.3 BTK inhibitors do not require BTK to lower inflammatory cytokines in murine macrophages

Drugs like ibrutinib and acalabrutinib are pharmacological agents which inhibit activity of BTK. In contrast, genetic ablation or gene mutation would delete the *Btk* gene or results in no functional BTK protein. In order to assess the difference between the two inhibitory approaches, we made use of two CBA-background mice strains. CBA/CaHN-Btk^{xid}/J mice have a point mutation in the *Btk* gene on the X-chromosome. The strains have a C-to-T substitution at coding nucleotide 82, which changes the codon 28 from an arginine to a cysteine (p.R28C).[69] We tested these mice alongside the CBA/CaJ strain as the closest wild-type controls of the same genetic background.[70] A random sample of these mice were genotyped using endpoint analysis method to validate their genetic background (Figure 6).

BMDMs were harvested from both CBA/CaJ (CBA-WT) and CBA/CaHN-BTK^{xid}/J (BTK-null) mice. These BMDMs were treated with optimized doses of ibrutinib (10 μM) or acalabrutinib (50 μM) for 22 hours, with LPS (200 ng/mL) added for the final 4 hours. As expected, we found that LPS alone stimulated a significant increase in the expression of *Il-1β*, *Il-6*, *Tnf*, and *Il-10* in cells derived from both strains (Figures 6A-B, 6D-E). The elevated expression of these four genes were significantly reduced by both ibrutinib and acalabrutinib treatment in cells derived from CBA-WT. Interestingly, in cells derived from the BTK-null strain, LPS induced *Il-1β*, *Tnf*, and *Il-10* expression similar to levels seen in the wild-type strain (Figure 7A, D-E). Further, ibrutinib and acalabrutinib treatment were able to significantly reduce the elevated expression in these genes. Taken together, the anti-inflammatory action of BTK inhibitors to lower transcription of

inflammatory cytokines do not require *Btk*. No significant differences were seen in Nlrp3 expression at any conditions between either strain (Figure 7C).

4.2.4 BTK inhibitors do not require BTK to mitigate inflammatory gene expression in macrophages after NLRP3 inflammasome activation

Building from our previous findings, BMDMs derived from both CBA-WT mice and BTK-null mice were treated with atorvastatin (1 μM) for 22 hours and either ibrutinib (10 μM) or acalabrutinib (50 μM), with LPS (200 ng/mL) added for the final 4 hours of treatment. The addition of atorvastatin induced significant increase in the expression of *Il-1β*, *Il-6*, *Tnf*, and *Il-10* relative to LPS only condition (Figure 8A, C-E). The results demonstrated that ibrutinib or acalabrutinib treatment significantly reduced the elevated expression of *Il-1β*, *Il-6*, *Tnf*, and *Il-10* relative to LPS and atorvastatin only conditions (Figure 8A, C-E).

We found that LPS and atorvastatin treatment elevated inflammatory gene expression to the same degree, both in cells derived from CBA-WT mice and cells of BTK-null mice. Furthermore, treatment with either of the two BTK inhibitors had a similar inhibitory effect on expression of *Il-1β*, *Il-6*, *Tnf*, and *Il-10* in BMDMs derived from both strains (Figure 8A, C-E). These results once again reinforce the idea that *Btk* is not required for the inhibitory effects of ibrutinib and acalabrutinib on inflammatory gene expression, regardless of the presence of an inflammasome activator like atorvastatin.

4.3 NLRP3 inflammasome activation in response to BTK inhibition

4.3.1 BTK inhibitors lower NLRP3 inflammasome-mediated IL-1β secretion in murine macrophages

Activation of the NLRP3 inflammasome promotes caspase-1-mediated cleavage and consequent secretion of mature IL-1β. We tested if BTK inhibitors altered IL-1β secretion from macrophages after exposure to the well-known NLRP3 inflammasome activator nigericin. BMDMs were prepared from either wild-type C57BL6/J mice (WT) or Nlrp3$^{-/-}$ mice. These cells were treated with ibrutinib (10 μM) or acalabrutinib (50 μM) for 22 hours, with LPS stimulation (200 ng/mL) for the final 4 hours, and nigericin (20 μM) added on 30 minutes before the end of treatment. The cell supernatants were collected for quantification of secreted cytokine levels. In WT-derived BMDMs, IL-1β secretion was only detectable in groups treated with both LPS and nigericin. The results show that LPS and nigericin treatment significantly increased IL-1β secretion from BMDMs. This elevation in IL-1β was significantly reduced when treated with either ibrutinib or acalabrutinib (Figure 9A). On the other hand, the LPS-nigericin-induced increase in IL-1β secretion does not occur in BMDMs derived from Nlrp3$^{-/-}$ mice, confirming the dependence of IL-1β secretion on an intact NLRP3 inflammasome, where IL-1β secretion was also undetectable in BMDMs derived from Nlrp3$^{-/-}$ mice treated with a BTK inhibitor (Figure 9A).

The same cell supernatants collected from the above experiment were also analyzed using an IL-6-specific ELISA to assess changes in an inflammatory cytokine that is not regulated by the NLRP3 inflammasome (Figure 9B). LPS alone was sufficient

to increase IL-6 in BMDMs from WT and Nlrp3$^{-/-}$ mice. Ibrutinib or acalabrutinib inhibited LPS-simulated IL-6 secretion in BMDMs from WT and Nlrp3$^{-/-}$ mice (Figure 9B).

4.3.2 BTK inhibitors do not require BTK to lower inflammasome-mediated IL-1β release

Given that BTK inhibitors did not require *Btk* to confer its inhibitory effects on inflammatory gene expression, we next tested if *Btk* was required for BTK inhibitors to alter inflammasome-mediated secretion of IL-1β. To address this question, we treated CBA-WT mice-derived and BTK-null mice-derived BMDMs with ibrutinib (10 μM) or acalabrutinib (50 μM) for 22 hours, with LPS stimulation (200 ng/mL) for the final 4 hours, and nigericin (20 μM) added on 30 minutes before the end of treatment. Media was collected from these samples to assess secretion of IL-1β and IL-6 by ELISA.

As expected, both LPS and nigericin are required for detectable levels of IL-1β release in BMDMs derived from CBA-WT and BTK-null mice. Treatment with ibrutinib (10 μM) and acalabrutinib (50 μM) significantly lowered IL-1β secretion in BMDMs derived from both strains of mice (Figure 10A). Similar results were obtained when these same samples were quantified with an IL-6-specific ELISA. As expected, LPS-alone was able to induce a significant increase in IL-6 secretion. The results showed that both ibrutinib and acalabrutinib significantly reduced the LPS- or LPS-nigericin-induced IL-6 secretion (Figure 10B). Taken together, these results demonstrate that BTK inhibitors have general anti-inflammatory properties that do not require *Btk*, but lower NLRP3 priming and activation, which extend to other pro-inflammatory cytokines such as IL-6 during LPS exposure.

4.4 Adipose tissue insulin signaling in response to BTK inhibitor treatment

4.4.1 Effect of BTK inhibitor treatment alone on adipose tissue insulin signaling

Henriksbo and colleagues have established that statin-induced activation of the NLRP3 inflammasome and the consequent IL-1β secretion leads to impaired insulin signaling in adipose tissue.[34] Stemming from these findings, we sought to test if BTK is involved in statin-induced insulin resistance in adipose tissue. To test this, we used an *ex vivo* model of murine adipose tissue explants extracted from wild-type C57BL/6J mice. The goal here was to optimize a model for testing the effect of BTK inhibition on adipose tissue insulin signaling *ex vivo*.

We wanted to determine if treatment of ibrutinib or acalabrutinib alone has any effect on adipose tissue insulin signaling. Here, adipose tissue explants were treated with various doses of ibrutinib (0.1-10 μM) or acalabrutinib (1-50 μM) for 22 hours, and insulin (0.3 nM) is added for the final 10 minutes of treatment to induce Akt phosphorylation. The phosphorylation status of Akt was analyzed as a marker of insulin signaling. The basal condition refers to untreated control without insulin exposure, while the control condition is also untreated but exposed to insulin stimulation. The control condition exhibited a significantly higher p-Akt/Akt ratio compared to the basal condition, which demonstrated that the insulin stimulation procedure was successful. We observed that ibrutinib or acalabrutinib at all tested doses did not significantly affect the p-Akt/Akt ratio of insulin-stimulated adipose tissue explants (Figure 11). This finding suggests that ibrutinib of up to 10 μM, and acalabrutinib of up to 50 μM can be added to this ex vivo model without a change in insulin sensitivity. This result paves the way for future

experiments to assess the effect of BTK inhibition on adipose tissue treated with a stressor (e.g., statins).

4.4.2 LPS as inflammasome primer in adipose tissue ex vivo

We determined the doses of ibrutinib and acalabrutinib that can be used in assessing the effect of BTK inhibition on insulin signaling. From here, we wanted to optimize an LPS dose to use as an inflammasome priming signal. We ideally want to find the maximum LPS dose that will not cause impaired insulin signaling. With this optimized dose, we would be able to add on an inflammasome activator (e.g., statin) as a stressor, and determine if BTK inhibition can alleviate the stressor-induced impairment in insulin signaling. To test this, we extracted adipose tissue explants from either CBA-WT or BTK-null mice. These explants were treated with ibrutinib (10 μM) in the presence of LPS-challenge (0.05, 0.5, 2 μg/mL, Figure 12A, 12C). This experiment was also performed with acalabrutinib (50 μM) in place of ibrutinib (Figure 12B, 12D).

In CBA-WT mice-derived adipose tissue explants, all tested doses of LPS had no significant effect on insulin signaling (Figure 12A, 12B). The addition of ibrutinib or acalabrutinib on these explants also did not alter insulin signaling. This result was also observed in BTK-null mice-derived adipose tissue explants, where neither of the two BTK inhibitors had a significant effect on insulin signaling, regardless of the presence of LPS at all tested doses (Figure 12C, 12D). Taken together, this experiment determined that LPS at concentrations up to 2 μg/mL can be used as an inflammasome priming agent without causing impairment in insulin signaling on its own. Along with the ideal doses of ibrutinib and acalabrutinib, we have optimized a model for accessing the effect of BTK inhibitors on NLRP3 inflammasome-mediated defects in adipose tissue insulin

signaling. This model will allow for testing if BTK inhibition is an effective approach to ameliorating statin-induced adipose tissue insulin resistance, previously established by Henriksbo and colleagues.[34]

4.4.3 Effect of BTK inhibition on bacterial cell wall-mediated insulin resistance in adipocytes

It is well-established that LPS acts as a ligand for TLR4 which induces an inflammatory response leading to the upregulation of numerous pro-inflammatory gene expression downstream.[19] Aside from TLR4, nucleotide oligomerization domain-containing proteins (NODs) are another common class of pattern recognition receptor of the innate immune system. NODs play a major role in obesity-related inflammation and metabolic dysfunction.[71,72] In particular activation of NOD1 with bacterial cell wall components can induce inflammation and promote dyslipidemia and insulin resistance in adipocytes.[20,73]

Aside from testing only LPS-mediated inflammation, we were interested in determining if the anti-inflammatory properties of BTK inhibitors can extend to NOD1-mediated insulin resistance in adipocytes. To test this, 3T3-L1 adipocytes were pre-incubated with either ibrutinib (10 µM) or acalabrutinib (50 µM) for 1 hour, before being exposed to FK-565 (10 µg/mL) for 48 hours to induce insulin resistance. Adipocytes were treated with insulin (100 nM) for the final 10 minutes to stimulate substantial Akt phosphorylation. The results demonstrated that stimulation with FK-565 significantly reduced Akt phosphorylation relative to insulin-stimulated control (Figure 13). Further, pre-incubation with ibrutinib, but not acalabrutinib, restored insulin signaling back to near-control levels. This finding shows that the BTK inhibitor Ibrutinib can attenuate cell-

autonomous insulin resistance cause by bacterial cell wall components. This finding suggests that the ability of ibrutinib to ameliorate NOD1-mediated insulin resistance may be different from acalabrutinib in adipocytes - and may pave the way to finding uniquely regulated kinases by these inhibitors.

5.0 DISCUSSION

The NLRP3 inflammasome is inherently a defensive mechanism of the innate immune system, design to sense metabolic danger signals and then mount a protective response. However, dysregulation in the form of a chronically inflammatory environment leads to maladaptive activation of the inflammasome. Over the past decade, many prominent immune and metabolic disorders like rheumatoid arthritis, Alzheimer's disease, atherosclerosis, type 2 diabetes, and insulin resistance, have converged at the NLRP3 inflammasome as a mediator of disease progression.[34,39,46,48] Extensive research efforts have gone into exploring this inflammasome, its components, and downstream effectors as therapeutic targets to address these conditions. The shortcoming of targeting inflammasome effectors like ASC or caspase-1 is that they are shared in the construction of several inflammasomes (other than NLRP3) and inflammatory pathways. Compounds developed to directly inhibit these effectors would increase the risk for cellular toxicity and opportunistic infections which would hinder the safety considerations of these potential drug candidates.[44] Several groups have achieved success in targeting IL-1 in an attempt to address NLRP3-mediated disorders. Anakinra, canakinumab, and rilonacept had shown promising efficacy in several autoimmune and inflammatory disorders.[45–47] Despite this success, therapeutic approaches via inhibition of IL-1β requires frequent and physically painful administration which leads to medication discontinuation. As well, the increased risk of opportunistic infection remains. To date, there has yet to be a clinically approved direct inhibitor of the NLRP3 inflammasome.

This challenge coincided with the timely publications by Ito et al. and Liu et al. where they positioned Bruton's tyrosine kinase as a regulator of NLRP3 and outlined the ability of BTK to regulate inflammasome-dependent production of IL-1β.[23,56] Since then, extensive efforts have gone into harnessing the potential of pharmacological BTK inhibition on ameliorating NLRP3 inflammasome-mediated diseases. Many groups have published positive findings on the therapeutic potential of BTK regulation in acute conditions like ischemic stroke, colitis, and even COVID-19.[56,60,74] Less research has focused on the implications of BTK inhibition on metabolic dysfunction. A recent paper by Purvis et al. thoroughly outlined the ability of ibrutinib treatment to address diet-induced metabolic inflammation *in vivo*.[66] Despite this, much remains unknown regarding the precise mechanism of action of these pharmacological inhibitors to confer these protective effects. Moreover, it remains unclear whether the efficacy of BTK inhibition extends to other triggers of metabolic inflammation, like impairment in insulin signaling induced by statins observed in adipose tissue by Henriksbo et al.[34] Therefore, it is critical to explore the mechanism of inhibitors like ibrutinib and acalabrutinib and their ability to ameliorate metabolic dysfunction induced by inflammasome-activating stressors like statins.

5.1 BTK inhibition lowers NLRP3 inflammasome priming and activation

Our efforts at uncovering the mechanism of action of BTK inhibitors, ibrutinib and acalabrutinib, began with an examination of how BTK regulates inflammatory gene expression. Through our experiments with the HEK-Blue Reporter System, we show both BTK inhibitors lower NF-κB activation during TLR4 and NOD1 stimulation. NF-κB is involved in inflammasome priming and many other inflammatory responses.[21] BTK

inhibitors had no effect in the absence of inflammation caused by microbial ligands (LPS, FK-565) that engage multiple types of pattern recognition receptors (TLR4, NOD1, respectively). These findings position BTK as a regulator of NLRP3 inflammasome priming, and many other inflammatory pathways by inhibiting NF-κB (Figure 14).

Given that NF-κB activation is a direct regulator of inflammatory and NLRP3 inflammasome effector gene expression, we next sought to determine the effect of BTK inhibition on the transcript levels of key inflammatory gene downstream. We have shown here that the tested BTK inhibitors alone can mitigate the elevation in inflammatory gene expression induced by LPS-priming in murine primary macrophages. We also showed that this effect occurs independent of statin exposure. These findings together provide solid evidence supporting the idea that BTK inhibitors alter the priming stage of the NLRP3 inflammasome mechanism, where transcription of inflammasome components like pro-IL-1β are upregulated. This result is inconsistent with the findings reported by Benner et al. which suggested that BTK inhibition specifically targets NLRP3 inflammasome activation, independent of priming.[65] They reported that although priming-induced IL-1β secretion is inhibited by BTK inhibitors, the *Il-1β* transcript levels were unchanged. This disparity may be attributed to the different cell type (BMDMs vs. tumour-associated macrophages) as well as difference in treatment protocol. Nevertheless, the results from our experiment strongly suggest that both ibrutinib and acalabrutinib alone can reduce the LPS-priming induced elevation in inflammatory gene expression. Since BTK inhibitors block LPS-induced priming, it is logical to hypothesize

that the inhibitor treatment would carry forward into downstream inflammasome-mediated consequences like lowering of IL-1β secretion.

Beyond inflammasome priming, we next determined if BTK inhibitors alter NLRP3 inflammasome activation, specifically the release of mature IL-1β. We found that treatment with ibrutinib or acalabrutinib lowered IL-1β secretion in LPS-primed macrophages stimulated by nigericin, a well-known inflammasome activator. As expected, IL-1β secretion was not increased in LPS-primed macrophages from mice lacking the *Nlrp3* gene. This demonstrates the necessity of NLRP3, and by extension – the inflammasome, in propagating IL-1β secretion and the inflammasome-inhibiting capability of BTK drug inhibitors. Consistent with our prior discoveries, the anti-inflammatory actions of Ibrutinib and Acalabrutinib extends beyond effectors of the NLRP3 inflammasome, as we observed that inhibitor treatment also led to a reduction in elevation of IL-6 release induced by extracellular stressor (LPS), where we confirmed that NLRP3 is not required for regulation of IL-6 (Figure 14).

5.2 Anti-inflammatory properties of BTK inhibition do not require BTK in macrophages

In our efforts to provide genetic validation for the observed effects produced by pharmacological BTK inhibitors on murine cells, we made use of the CBA/CaHN-Btk^{xid}/J mice strain as a BTK-null model. A strength of our results on BTK inhibitors is that the observed effects were reproducible in primary cells derived from 3 mouse strains, including CBA/CaHN-Btk^{xid}/J, CBA/CaJ and C57BL/6J mice. We discovered that both BTK inhibitors tested could reduce LPS-induced elevations in expression of multiple inflammatory markers (*Il-1β*, *Tnf*, *Il-10*). Given that these effects were consistently

observed in primary macrophages irrespective of the presence of the BTK gene, these results suggest that the anti-inflammatory action of ibrutinib and acalabrutinib operate through a BTK-independent mechanism (Figure 14). Taken together, these findings suggest that the anti-inflammatory effects of BTK inhibitors do not require an inflammasome activation signal and BTK inhibitors can lower inflammation in the absence of BTK. In addition, even in the presence of a well-known NLRP3 inflammasome activator, nigericin, BTK inhibitors can lower IL-1β secretion, which again occurred in macrophages that lack the BTK gene. Hence, BTK inhibitors have widespread anti-inflammatory properties that extend to the NLRP3 inflammasome and beyond, but do not require BTK.

The clinical feasibility of repurposing ibrutinib beyond its therapeutic properties in B cell malignancies has largely been slowed due to its well-established off-target toxicities. Long-term toxicity profile of ibrutinib includes substantial incidence of atrial fibrillation, hypertension, bleeding, infection, among other adverse events.[75] This risk adverse off-target effects justified the further development of next-generation BTK inhibitors, specifically designed to target BTK with a higher specificity. Acalabrutinib, though it has a slightly higher IC_{50}, it binds less potently to other cysteine-containing kinases similar to BTK.[64] Perhaps the most unexpected finding in this thesis was that neither ibrutinib nor acalabrutinib require BTK for confer the anti-inflammatory properties we observed in our gene expression and inflammasome activation experiments. This finding would imply that these specific anti-inflammatory actions are mediated through off-target nodes/pathway that are shared between the two BTK inhibitors.

As a preliminary attempt to sieve through the off-target candidates of both BTK inhibitors, we referenced two separate studies that screened for the kinase binding profiles of ibrutinib and acalabrutinib.[76,77] Both studies obtained these screens through a platform known as KINOMEscan® by DiscoverRX. This platform is an ATP active site-directed competition binding assay that is run for a particular compound of interest (ibrutinib/acalabrutinib in this case) against a library of approximately 300-400 kinases.[78] For each of these studies, the compound of interest was tested at a concentration of 1 µM against the panel of kinases. The results are presented as a "percentage of control" value, where 100% means no inhibition of kinase binding in the presence of the compound of interest, and 0% means complete inhibition of kinase binding. We have collated the results from both studies and generated a chart of common kinase targets and the associated percentage of control values in the presence of ibrutinib or acalabrutinib (Table 4).

According to the kinase binding profiles, it is apparent that both Ibrutinib and Acalabrutinib substantially inhibit other members of the Tec family tyrosine kinases, namely, tyrosine-protein kinases (TEC, TXK), bone marrow tyrosine kinase on chromosome X (BMX). TEC and TXK are both predominantly expressed in T-cells and play intricate roles in regulating the differentiation and signal transduction of specific subtypes of T-cells. BMX, on the other hand, is expressed in hematopoietic cells of the myeloid lineage. Gene silencing against Bmx demonstrated lowering of LPS-induced IL-6 secretion in synovial fibroblasts.[79] BMX overexpression is also observed in inflammatory disorders like rheumatoid arthritis and neuronal ischemia, and suppression of BMX demonstrated protection.[79,80] Transient removal of BMX in human fibroblasts

stimulated by TNFα and IL-1β significantly improves recruitment of IL-8, a potent neutrophil attractant directed to inflammatory sites.[81,82] In regards to TLR4 receptor signaling, it was shown that activated BMX interacts with components of the MyD88-dependent pathway of signal transduction (MyD88, Mal).[83] As well, BMX is required for phosphorylation of downstream TLR4 effectors, p38 mitogen-activated protein kinase, cJun N-terminal kinase (JNK), and NF-κB.[84,85] Its intimate involvement with inflammatory cytokines and TLR4-signaling posits BMX as a node inhibited by both ibrutinib and acalabrutinib that potentially mediates the observed anti-inflammatory properties.

Another family of kinases that were strongly inhibited by ibrutinib and acalabrutinib was epidermal growth factor receptor (EGFR) family kinases. Specifically, ErbB receptor 2 and 4 (ErbB2, ErbB4) were strongly inhibited by both BTK inhibitors.

ErbB2 stabilizes other EGFRs ligand binding and enhance signaling. It is also overexpressed in a significant portion of non-small cell lung cancer cases.[86] In a lung-specific ErbB2-overexpressing transgenic mouse model, it was observed that, concurrent with worsening of pulmonary cancer progression, several inflammatory factors like TNFα, IL-1β, and IL-6 were upregulated in lung tissues.[86] Inhibition of ErbB2 would reduce the abundance of these inflammatory cytokines. However, these results are only relevant in lung tissues, and thus a more systemic look at the effects of ErbB2 inhibition is required.

ErbB4 is a transmembrane receptor protein essential to cell surface recognition of neuregulins, which are signaling proteins that mediate cellular functions of the neuronal system. ErbB4 has been linked to pro-inflammatory macrophage activity.[87]

Treatment with ErbB4 ligand neuregulin-4 (NRG4) induces apoptosis in activated pro-inflammatory macrophages.[87] In a murine colitis model, it was shown that inflammation suppressed NRG4 expression which allowed for the persistence of activated pro-inflammatory macrophages. By ablating either the ErbB4 receptor or its ligand NRG4, an elevated abundance of pro-inflammatory cytokines was observed in activated macrophages.[88] The inherently protective effect against inflammation mediated by NRG4 and ErbB4 would suggest that its inhibition would lead to exacerbated pro-inflammatory outcomes. However, these findings were studied in the context of intestinal inflammation and colitis, so further efforts are required to validate that ErbB4 is not involved in mediating the observed anti-inflammatory properties of ibrutinib and acalabrutinib.

5.3 Optimized conditions for testing BTK inhibition on adipose tissue insulin signaling ex vivo

Further, to develop our model of testing adipose tissue insulin signaling *ex vivo*, we sought out to understand if treatment of ibrutinib and acalabrutinib alone impairs insulin signaling. We here demonstrated that in C57BL6/J mice, the two drug inhibitors tested do not have a significant effect on insulin-stimulated adipose tissue explants, as shown by the consistent phosphorylation status of insulin signaling at the level of Akt. Moreover, we have results demonstrating that LPS at concentrations up to 2 µg/mL can be added to the explants as an inflammasome priming signal without inducing a significant change on insulin signaling. This completes our optimized *ex vivo* model for us to test drug interventions or stress-induction without any concerns of artefact attributed to LPS or the two drug inhibitors alone. Given the compelling results we have

presented on BTK inhibitors lowering LPS and statin-induced inflammatory gene expression, we are now in a position to test if BTK inhibitors can mitigate insulin resistance in adipose tissue induced by inflammasome activators like statins.

5.4 Future Directions

We have shown here that BTK inhibitors, ibrutinib and acalabrutinib, are able to reduce NLRP3 inflammasome-mediated inflammatory gene expression and cytokine secretion. Along with results published by Purvis et al., BTK inhibitor treatment has emerged as a promising therapeutic approach to combat stress-induced metabolic inflammation.[66] As well, we have developed an optimized protocol for testing the effectiveness of BTK inhibition on insulin signaling in adipose tissue *ex vivo*. All these efforts set the stage for a future experiment to determine the efficacy of BTK inhibition on improving statin-induced insulin resistance in adipose tissue. By stimulating these explants with LPS along with a statin, we would expect a significant reduction in the phosphorylation of Akt, indicative of impairment in insulin signaling, just as previously established by Henriksbo et al.[34] With the addition of ibrutinib or acalabrutinib, the results will reveal whether the anti-inflammatory properties presented throughout this thesis is sufficient to rescue statin-induced metabolic dysfunction in adipose tissue.

We have also presented in this thesis the unexpected discovery that the anti-inflammatory properties of ibrutinib and acalabrutinib do not require BTK. Considering that this observed effect was consistent between ibrutinib and acalabrutinib treatment, it would suggest that this is attributed to an off-target node shared between the two drug inhibitors. This finding prompts us towards another future direction to identify the off-target responsible for conferring these BTK-independent effects. Collating the kinase

binding profile of ibrutinib and acalabrutinib into Table 4 is only the first step. We next intend to sift through this dataset to narrow down potential off-target kinases that are inhibited to a substantial degree by both ibrutinib and acalabrutinib. From there, we can employ targeted approaches to inhibit these potential kinase candidates to determine if they are required for the observed ibrutinib/acalabrutinib effects.

Predicated on the potential success of BTK inhibitors to ameliorate statin-induced adipose tissue insulin resistance *ex vivo*, another possible future direction would be to test the effect of BTK inhibitor administration in an *in vivo* statin-induced dysglycemia model. Our lab has previously discovered that feeding a fluvastatin-laden diet (500 mg/kg in food) increases blood glucose during a glucose tolerance test in obese *ob/ob* (leptin-deficient) mice or in high-fat diet (HFD) fed C57BL/6J mice (unpublished). This study would require feeding CBA-WT and BTK-null mice one of four diets: 1) chow diet, 2) statin-laden chow diet, 3) HFD diet, 4) statin-laden HFD diet. Once the dysglycemia phenotype is confirmed by oral glucose tolerance test, ibrutinib or acalabrutinib can be administered via oral gavage as demonstrated by Purvis et al. in their 2020 publication. This experiment would reveal if the anti-inflammatory of BTK inhibitors can extend to metabolic dysregulation in an *in vivo* mice model.

5.5 Limitations

One of the limitations to this thesis is the absence of cell viability determination in experiments involving HEK-293T and BMDMs. Cell viability of these cell types following treatment with one or more of: LPS, FK-565, atorvastatin, ibrutinib and acalabrutinib, was not quantitatively determined. This control experiment should be performed to

verify that the observed inflammatory responses were indeed a consequence of the experimental treatment, rather than artefact of cell death.

As well, a portion of the inflammatory gene expression data was normalized to LPS-only conditions, while another was normalized to untreated control.

Another important limitation to this thesis is the ambiguous distribution of adipose tissue explant content. Due to the nature of tissue explant preparation, it is not possible to normalize the exact amount of explant that is distributed into each experiment group. During the experiment, we do our best to maintain an internal standard for the size of explant to be allocated to each individual sample, however, this measure is qualitative at best. One potential way to address this concern would be to dry each adipose tissue fat pad and weigh out an exact amount of tissue content for each individual sample. However, the drawback to this approach would be that keeping tissue *ex vivo* and deprived of nutrients for an extended period of time could affect tissue viability.

Moreover, to test a model of *Btk* ablation, we used two CBA-background strains. Since these mice strains are not commonly purchased, the provider (The Jackson Laboratory) only maintains a small colony with limited availability in terms of ages. For the purposes of the experiments outlined in this thesis, we had to use age-matched mice of both the CBA/CaJ and CBA/CaHN-Btk^{xid}/J strains for each experiment. The low availability became a hindrance as often, The Jackson Laboratory would only be able to offer age-matched mice at very young ages. This meant that our experimental timeline was dictated by and delayed due to the availability of these mice strains.

Lastly, I was fortunate enough to be able to continue my graduate studies during the COVID-19 pandemic. However, during the early months of my masters, most laboratories, including ours, were limited by restrictions. For months, this meant that only three lab members could physically be working at a time. These restrictions not only slowed initial training, but also progression of experiments.

6.0 CONCLUSION

The postulation that BTK is a direct regulator of NLRP3 inflammasome function is a growing field of interest. Despite the ongoing efforts, the tissue-specific metabolic consequences of BTK inhibition downstream of the NLRP3 inflammasome remains unclear. Specifically, the effect of BTK inhibition on insulin signaling in metabolic tissues is largely unstudied. This was a key knowledge gap given the broad range of inflammatory disorders that engage the NLRP3 inflammasome in their pathogenesis and progression. As well, the lack of a clinically approved direct inhibitor of the inflammasome calls for innovative approaches to regulate this node of innate immunity. Here, we demonstrate that pharmacological inhibition of BTK lowers NLRP3 inflammasome priming and activation. Further, we made the serendipitous discovery that these BTK inhibitors have anti-inflammatory properties that do not require the presence of the *Btk* gene product. This intriguing finding encourages the search for off-targets shared between ibrutinib and acalabrutinib that may potentially act as the mediator of the observed anti-inflammatory effects. We have also optimized the experimental conditions for testing the effects of BTK inhibition on the NLRP3 inflammasome using an *ex vivo* adipose tissue model. An important future direction is to explore the efficacy of BTK inhibition as a therapeutic approach to ameliorating tissue-localized insulin resistance induced by activators of the NLRP3 inflammasome. Pinpointing the off-target responsible for its anti-inflammatory properties would posit BTK inhibitors as effective inhibitors of NLRP3 inflammasome function and present them as efficacious treatment options for a myriad of inflammatory diseases.

7.0 REFERENCES

1. Saeedi P, Petersohn I, Salpea P, et al. Global and regional diabetes prevalence estimates for 2019 and projections for 2030 and 2045: Results from the International Diabetes Federation Diabetes Atlas, 9th edition. *Diabetes Res Clin Pract*. 2019;157. doi:10.1016/j.diabres.2019.107843

2. DeFronzo RA, Ferrannini E, Groop L, et al. Type 2 diabetes mellitus. *Nat Rev Dis Prim*. 2015;1. doi:10.1038/nrdp.2015.19

3. Swinburn BA, Kraak VI, Allender S, et al. The Lancet Commissions The Global Syndemic of Obesity, Undernutrition, and Climate Change: The Lancet Commission report. *www.thelancet.com*. 2019;393:791. doi:10.1016/S0140-6736(18)32822-8

4. Bancej C, Jayabalasingham ; B, Wall ; R W, et al. Evidence Brief Trends and projections of obesity among Canadians. http://apps.who. Accessed July 24, 2022.

5. Haffner S, Taegtmeyer H. Epidemic obesity and the metabolic syndrome. *Circulation*. 2003;108(13):1541-1545. doi:10.1161/01.CIR.0000088845.17586.EC

6. Shulman GI. Ectopic Fat in Insulin Resistance, Dyslipidemia, and Cardiometabolic Disease. *N Engl J Med*. 2014;371(12):1131-1141. doi:10.1056/nejmra1011035

7. Reardon CA, Shibata R, Akasaki Y, Den Hartigh LJ, Chait A. Adipose Tissue Distribution, Inflammation and Its Metabolic Consequences, Including Diabetes and Cardiovascular Disease. *Front Cardiovasc Med* | *www.frontiersin.org*. 2020;7:22. doi:10.3389/fcvm.2020.00022

8. Antuna-Puente B, Feve B, Fellahi S, Bastard J-P. Adipokines: The missing link between insulin resistance and obesity. *Diabetes Metab*. 2008;34:2-11. doi:10.1016/j.diabet.2007.09.004

9. Hotamisligil GS, Shargill NS, Spiegelman BM. Adipose expression of tumor necrosis factor-α: Direct role in obesity-linked insulin resistance. *Science (80-)*. 1993;259(5091):87-91. doi:10.1126/science.7678183

10. Hotamisligil GS. Inflammation, metaflammation and immunometabolic disorders. *Nature*. 2017;542(7640):177-185. doi:10.1038/nature21363

11. Lancaster GI, Langley KG, Berglund NA, et al. Evidence that TLR4 Is Not a Receptor for Saturated Fatty Acids but Mediates Lipid-Induced Inflammation by Reprogramming Macrophage Metabolism. *Cell Metab*. 2018;27(5):1096-1110.e5. doi:10.1016/j.cmet.2018.03.014

12. Nguyen MTA, Favelyukis S, Nguyen AK, et al. A subpopulation of macrophages infiltrates hypertrophic adipose tissue and is activated by free fatty acids via toll-like receptors 2 and 4 and JNK-dependent pathways. *J Biol Chem*. 2007;282(48):35279-35292. doi:10.1074/jbc.M706762200

13. Ré Mie Boucher J, Kleinridders A, Kahn CR. Insulin Receptor Signaling in Normal and Insulin-Resistant States. doi:10.1101/cshperspect.a009191

14. McPhee JB, Schertzer JD. Immunometabolism of obesity and diabetes: Microbiota link compartmentalized immunity in the gut to metabolic tissue inflammation. *Clin Sci*. 2015;129(12):1083-1096. doi:10.1042/CS20150431

15. Mehran AE, Templeman NM, Brigidi GS, et al. Hyperinsulinemia drives diet-induced obesity independently of brain insulin production. *Cell Metab*. 2012;16(6):723-737. doi:10.1016/J.CMET.2012.10.019

16. Tsai S, Clemente-Casares X, Zhou AC, et al. Insulin Receptor-Mediated Stimulation Boosts T Cell Immunity during Inflammation and Infection. *Cell Metab*. 2018;28(6):922-

934.e4. doi:10.1016/j.cmet.2018.08.003

17. Horiguchi H, Loftus TJ, Hawkins RB, et al. Innate immunity in the persistent inflammation, immunosuppression, and catabolism syndrome and its implications for therapy. *Front Immunol*. 2018;9(APR). doi:10.3389/fimmu.2018.00595

18. Kawai T, Akira S. The role of pattern-recognition receptors in innate immunity: Update on toll-like receptors. *Nat Immunol*. 2010;11(5):373-384. doi:10.1038/ni.1863

19. Poltorak A, He X, Smirnova I, et al. Defective LPS signaling in C3H/HeJ and C57BL/10ScCr mice: Mutations in Tlr4 gene. *Science (80-)*. 1998;282(5396):2085-2088. doi:10.1126/science.282.5396.2085

20. Schertzer JD, Tamrakar AK, Magalhães JG, et al. NOD1 Activators Link Innate Immunity to Insulin Resistance. *Diabetes*. 2011;60:2206-2215. doi:10.2337/db11-0004

21. Jo EK, Kim JK, Shin DM, Sasakawa C. Molecular mechanisms regulating NLRP3 inflammasome activation. *Cell Mol Immunol*. 2016;13(2):148-159. doi:10.1038/cmi.2015.95

22. Barra NG, Henriksbo BD, Anhê FF, Schertzer JD. The NLRP3 inflammasome regulates adipose tissue metabolism. *Biochem J*. 2020;477(6):1089-1107. doi:10.1042/BCJ20190472

23. Liu X, Pichulik T, Wolz OO, et al. Human NACHT, LRR, and PYD domain–containing protein 3 (NLRP3) inflammasome activity is regulated by and potentially targetable through Bruton tyrosine kinase. *J Allergy Clin Immunol*. 2017;140(4):1054-1067.e10. doi:10.1016/j.jaci.2017.01.017

24. Haneklaus M, O'Neill LAJ, Coll RC. Modulatory mechanisms controlling the NLRP3 inflammasome in inflammation: Recent developments. *Curr Opin Immunol*.

2013;25(1):40-45. doi:10.1016/j.coi.2012.12.004

25. McBride MJ, Foley KP, D'Souza DM, et al. The NLRP3 inflammasome contributes to sarcopenia and lower muscle glycolytic potential in old mice. *Am J Physiol Metab*. 2017;313(2):E222-E232. doi:10.1152/ajpendo.00060.2017

26. Shao W, Yeretssian G, Doiron K, Hussain SN, Saleh M. The Caspase-1 Digestome Identifies the Glycolysis Pathway as a Target during Infection and Septic Shock * □ S. 2007. doi:10.1074/jbc.M708182200

27. Zhang SY, Dong YQ, Wang P, et al. Adipocyte-derived Lysophosphatidylcholine Activates Adipocyte and Adipose Tissue Macrophage Nod-Like Receptor Protein 3 Inflammasomes Mediating Homocysteine-Induced Insulin Resistance. *EBioMedicine*. 2018;31:202-216. doi:10.1016/j.ebiom.2018.04.022

28. Wen H, Gris D, Lei Y, et al. Fatty acid-induced NLRP3-ASC inflammasome activation interferes with insulin signaling. *Nat Immunol*. 2011;12(5):408-415. doi:10.1038/ni.2022

29. Yang Y, Wang H, Kouadir M, Song H, Shi F. Recent advances in the mechanisms of NLRP3 inflammasome activation and its inhibitors. *Cell Death Dis*. 2019;10(2):1-11. doi:10.1038/s41419-019-1413-8

30. Murakami T, Ockinger J, Yu J, et al. Critical role for calcium mobilization in activation of the NLRP3 inflammasome. *Proc Natl Acad Sci U S A*. 2012;109(28):11282-11287. doi:10.1073/pnas.1117765109

31. Zhong Z, Liang S, Sanchez-Lopez E, et al. New mitochondrial DNA synthesis enables NLRP3 inflammasome activation. *Nature*. 2018;560(7717):198-203. doi:10.1038/s41586-018-0372-z

32. Bruun JM, Stallknecht B, Helge JW, Richelsen B. Interleukin-18 in plasma and adipose

tissue: effects of obesity, insulin resistance, and weight loss. *Eur J Endocrinol*. 157:465-471. doi:10.1530/EJE-07-0206

33. Henriksbo BD, Lau TC, Cavallari JF, et al. Fluvastatin causes NLRP3 inflammasome-mediated adipose insulin resistance. *Diabetes*. 2014;63(11):3742-3747. doi:10.2337/db13-1398

34. Henriksbo BD, Tamrakar AK, Xu J, et al. Statins promote interleukin-1β-dependent adipocyte insulin resistance through lower prenylation, not cholesterol. *Diabetes*. 2019;68(7):1441-1448. doi:10.2337/db18-0999

35. Henriksbo BD, Tamrakar AK, Phulka JS, Barra NG, Schertzer JD. Statins activate the NLRP3 inflammasome and impair insulin signaling via p38 and mTOR. *Am J Physiol - Endocrinol Metab*. 2020;319(1):E110-E116. doi:10.1152/ajpendo.00125.2020

36. Tartey S, Kanneganti T-D. Inflammasomes in the Pathophysiology of Autoinflammatory Syndromes. doi:10.1002/JLB.3MIR0919-191R

37. Jankovic D, Ganesan J, Bscheider M, et al. The Nlrp3 inflammasome regulates acute graft-versus-host disease. *J Exp Med*. 2013;210(10):1899. doi:10.1084/JEM.20130084

38. Kim HY, Lee HJ, Chang Y-J, et al. IL-17 producing innate lymphoid cells and the NLRP3 inflammasome facilitate obesity-associated airway hyperreactivity HHS Public Access Author manuscript. *Nat Med*. 2014;20(1):54-61. doi:10.1038/nm.3423

39. Heneka MT, Kummer MP, Stutz A, et al. NLRP3 is activated in Alzheimer´s disease and contributes to pathology in APP/PS1 mice. *Nature*. 2013;493(7434):674. doi:10.1038/NATURE11729

40. Vandanmagsar B, Youm Y-H, Ravussin A, et al. The NALP3/NLRP3 Inflammasome Instigates Obesity-Induced Autoinflammation and Insulin Resistance HHS Public Access.

Nat Med. 2011;17(2):179-188. doi:10.1038/nm.2279

41. Lee H-M, Kim J-J, Kim HJ, Shong M, Ku BJ, Jo E-K. Upregulated NLRP3 Inflammasome Activation in Patients With Type 2 Diabetes. doi:10.2337/db12-0420

42. Stienstra R, van Diepen JA, Tack CJ, et al. Inflammasome is a central player in the induction of obesity and insulin resistance. doi:10.1073/pnas.1100255108

43. Stienstra R, Joosten LAB, Koenen T, et al. The inflammasome-mediated caspase-1 activation controls adipocyte differentiation and insulin sensitivity. *Cell Metab*. 2010;12(6):593-605. doi:10.1016/J.CMET.2010.11.011

44. Mangan MSJ, Olhava EJ, Roush WR, Seidel HM, Glick GD, Latz E. Targeting the NLRP3 inflammasome in inflammatory diseases. *Nat Rev Drug Discov 2018 178*. 2018;17(8):588-606. doi:10.1038/nrd.2018.97

45. Jesus AA, Goldbach-Mansky R. IL-1 Blockade in Autoinflammatory Syndromes. *Annu Rev Med*. 2014;65:223. doi:10.1146/ANNUREV-MED-061512-150641

46. Calabrese LH, Nazario M, Parent M. Anakinra treatment of patients with rheumatoid arthritis. *Ann Pharmacother*. 2002;36(7-8):1204-1209. doi:10.1345/aph.1A396

47. Chakraborty A, Tannenbaum S, Rordorf C, et al. Pharmacokinetic and Pharmacodynamic Properties of Canakinumab, a Human Anti-Interleukin-1β Monoclonal Antibody. *Clin Pharmacokinet*. 2012;51(6):e1. doi:10.2165/11599820-000000000-00000

48. Ridker PM, Everett BM, Thuren T, et al. Antiinflammatory Therapy with Canakinumab for Atherosclerotic Disease. *N Engl J Med*. 2017;377(12):1119-1131. doi:10.1056/NEJMOA1707914/SUPPL_FILE/NEJMOA1707914_DISCLOSURES.PDF

49. Ridker PM, Thuren T, Zalewski A, Libby P. Interleukin-1β inhibition and the prevention of recurrent cardiovascular events: rationale and design of the Canakinumab Anti-

inflammatory Thrombosis Outcomes Study (CANTOS). *Am Heart J*. 2011;162(4):597-605. doi:10.1016/J.AHJ.2011.06.012

50. Coll RC, Hill JR, Day CJ, et al. MCC950 directly targets the NLRP3 ATP-hydrolysis motif for inflammasome inhibition. *Nat Chem Biol 2019 156*. 2019;15(6):556-559. doi:10.1038/s41589-019-0277-7

51. Coll RC, Robertson AAB, Chae JJ, et al. A small molecule inhibitior of the NLRP3 inflammasome is a potential therapeutic for inflammatory diseases. *Nat Med*. 2015;21(3):248. doi:10.1038/NM.3806

52. Vetrie D, Vořechovský I, Sideras P, et al. The gene involved in X-linked agammaglobulinaemia is a member of the src family of protein-tyrosine kinases. *Nature*. 1993;361(6409):226-233. doi:10.1038/361226a0

53. Weber ANR, Bittner Z, Liu X, Dang TM, Radsak MP, Brunner C. Bruton's tyrosine kinase: An emerging key player in innate immunity. *Front Immunol*. 2017;8(NOV). doi:10.3389/fimmu.2017.01454

54. Pal Singh S, Dammeijer F, Hendriks RW. Role of Bruton's tyrosine kinase in B cells and malignancies. *Mol Cancer*. 2018;17(1). doi:10.1186/s12943-018-0779-z

55. Weber ANR. Targeting the NLRP3 Inflammasome via BTK. *Front cell Dev Biol*. 2021;9. doi:10.3389/FCELL.2021.630479

56. Ito M, Shichita T, Okada M, et al. Bruton's tyrosine kinase is essential for NLRP3 inflammasome activation and contributes to ischaemic brain injury. *Nat Commun*. 2015;6. doi:10.1038/ncomms8360

57. Burger JA, Tedeschi A, Barr PM, et al. Ibrutinib as Initial Therapy for Patients with Chronic Lymphocytic Leukemia. *N Engl J Med*. 2015;373(25):2425-2437.

doi:10.1056/nejmoa1509388

58. Chang BY, Huang MM, Francesco M, et al. The Bruton tyrosine kinase inhibitor PCI-32765 ameliorates autoimmune arthritis by inhibition of multiple effector cells. *Arthritis Res Ther*. 2011;13(4). doi:10.1186/ar3400

59. Ito M, Shichita T, Okada M, et al. ARTICLE Bruton's tyrosine kinase is essential for NLRP3 inflammasome activation and contributes to ischaemic brain injury. 2015. doi:10.1038/ncomms8360

60. Mao L, Kitani A, Hiejima E, et al. Bruton tyrosine kinase deficiency augments NLRP3 inflammasome activation and causes IL-1β-mediated colitis. *J Clin Invest*. 2020;130(4):1793-1807. doi:10.1172/JCI128322

61. Honigberg LA, Smith AM, Sirisawad M, et al. The Bruton tyrosine kinase inhibitor PCI-32765 blocks B-cell activation and is efficacious in models of autoimmune disease and B-cell malignancy. *Proc Natl Acad Sci U S A*. 2010;107(29):13075-13080. doi:10.1073/pnas.1004594107

62. Levade M, David E, Garcia C, et al. Ibrutinib treatment affects collagen and von Willebrand factor-dependent platelet functions. *Blood*. 2014;124(26):3991-3995. doi:10.1182/blood-2014-06-583294

63. Kamel S, Horton L, Ysebaert L, et al. Ibrutinib inhibits collagen-mediated but not ADP-mediated platelet aggregation. *Leukemia*. 2015;29(4):783-787. doi:10.1038/leu.2014.247

64. Patel V, Balakrishnan K, Bibikova E, et al. Comparison of acalabrutinib, a selective Bruton tyrosine kinase inhibitor, with ibrutinib in chronic lymphocytic leukemia cells. *Clin Cancer Res*. 2017;23(14):3734-3743. doi:10.1158/1078-0432.CCR-16-1446

65. Benner B, Scarberry L, Stiff A, et al. Evidence for interaction of the NLRP3 inflammasome

and Bruton's tyrosine kinase in tumor-associated macrophages: implications for myeloid cell production of interleukin-1beta. *Oncoimmunology*. 2019;8(11). doi:10.1080/2162402X.2019.1659704

66. Purvis GSD, Collino M, Haidee Aranda-Tavio |, et al. Inhibition of Bruton's TK regulates macrophage NF-κB and NLRP3 inflammasome activation in metabolic inflammation. 2020. doi:10.1111/bph.15182

67. Bittner ZA, Liu X, Tortola MM, et al. BTK operates a phospho-tyrosine switch to regulate NLRP3 inflammasome activity. *J Exp Med*. 2021;218(11). doi:10.1084/JEM.20201656/212658

68. Saban MR, Hellmich H, Nguyen NB, Winston J, Hammond TG, Saban R. Time course of LPS-induced gene expression in a mouse model of genitourinary inflammation. *Physiol Genomics*. 2001;2001(5):147-160. doi:10.1152/PHYSIOLGENOMICS.2001.5.3.147/SUPPL_FILE/FIG8C.JPG

69. 001011 - CBA/CaHN-Btk<xid>/J. https://www.jax.org/strain/001011. Accessed September 1, 2021.

70. 000654 - CBA/Ca Strain Details. https://www.jax.org/strain/000654. Accessed March 25, 2022.

71. Chi W, Dao D, Lau TC, et al. Bacterial Peptidoglycan Stimulates Adipocyte Lipolysis via NOD1. *PLoS One*. 2014;9(5):e97675. doi:10.1371/JOURNAL.PONE.0097675

72. Denou E, Lolmède K, Garidou L, et al. Defective NOD2 peptidoglycan sensing promotes diet-induced inflammation, dysbiosis, and insulin resistance. *EMBO Mol Med*. 2015;7(3):259-274. doi:10.15252/EMMM.201404169

73. Zhao L, Hu P, Zhou Y, Purohit J, Hwang D. NOD1 activation induces proinflammatory

gene expression and insulin resistance in 3T3-L1 adipocytes. *Am J Physiol - Endocrinol Metab*. 2011;301(4):587-598. doi:10.1152/AJPENDO.00709.2010

74. Roschewski M, Lionakis MS, Sharman JP, et al. Inhibition of Bruton tyrosine kinase in patients with severe COVID-19. *Sci Immunol*. 2020;5(48):110. doi:10.1126/SCIIMMUNOL.ABD0110/SUPPL_FILE/ABD0110_SM_TABLE_S11.XLSX

75. Byrd JC, Furman RR, Coutre SE, et al. Ibrutinib Treatment for First-Line and Relapsed/Refractory Chronic Lymphocytic Leukemia: Final Analysis of the Pivotal Phase Ib/II PCYC-1102 Study HHS Public Access. *Clin Cancer Res*. 2020;26(15):3918-3927. doi:10.1158/1078-0432.CCR-19-2856

76. Ibrutinib KINOMEscan - Dataset - HMS LINCS Database - HMS LINCS Project. https://lincs.hms.harvard.edu/db/datasets/20222/main. Accessed July 27, 2022.

77. Herman SEM, Montraveta A, Niemann CU, et al. The Bruton's tyrosine kinase (BTK) inhibitor acalabrutinib demonstrates potent on-target effects and efficacy in two mouse models of chronic lymphocytic leukemia. *Clin Cancer Res*. 2017;23(11):2831. doi:10.1158/1078-0432.CCR-16-0463

78. Fabian MA, Biggs WH, Treiber DK, et al. A small molecule–kinase interaction map for clinical kinase inhibitors. *Nat Biotechnol 2005 233*. 2005;23(3):329-336. doi:10.1038/nbt1068

79. Palmer CD, Mutch BE, Workman S, McDaid JP, Horwood NJ, Foxwell BMJ. Bmx tyrosine kinase regulates TLR4-induced IL-6 production in human macrophages independently of p38 MAPK and NFkapp}B activity. *Blood*. 2008;111(4):1781-1788. doi:10.1182/BLOOD-2007-07-102343

80. Chen KY, Wu CC, Chang CF, et al. Suppression of Etk/Bmx protects against ischemic

brain injury. *Cell Transplant*. 2012;21(1):345-354. doi:10.3727/096368911X582741

81. Nakagome K, Matsushita S, Nagata M. Neutrophilic inflammation in severe asthma. *Int Arch Allergy Immunol*. 2012;158 Suppl 1(SUPPL. 1):96-102. doi:10.1159/000337801

82. Qiu L, Wang F, Liu S, Chen XL. Current understanding of tyrosine kinase BMX in inflammation and its inhibitors. *Burn Trauma*. 2014;2(3):121-124. doi:10.4103/2321-3868.135483

83. Semaan N, Alsaleh G, Gottenberg J-E, Wachsmann D, Sibilia J. Etk/BMX, a Btk family tyrosine kinase, and Mal contribute to the cross-talk between MyD88 and FAK pathways. *J Immunol*. 2008;180(5):3485-3491. doi:10.4049/JIMMUNOL.180.5.3485

84. Guo L, Guo Y, Xiao S. Expression of tyrosine kinase Etk/Bmx and its relationship with AP-1- and NF-kappaB-associated proteins in hepatocellular carcinoma. *Oncology*. 2007;72(5-6):410-416. doi:10.1159/000113491

85. Gottar-Guillier M, Dodeller F, Huesken D, et al. The tyrosine kinase BMX is an essential mediator of inflammatory arthritis in a kinase-independent manner. *J Immunol*. 2011;186(10):6014-6023. doi:10.4049/JIMMUNOL.1002813

86. Zeng S, Yang Y, Tan Y, et al. ERBB2-induced inflammation in lung carcinogenesis. *Mol Biol Rep*. 2012;39(8):7911-7917. doi:10.1007/s11033-012-1635-7

87. Schumacher MA, Hedl M, Abraham C, et al. ErbB4 signaling stimulates pro-inflammatory macrophage apoptosis and limits colonic inflammation. *Cell Death Dis*. 2017;8(2):e2622. doi:10.1038/CDDIS.2017.42

88. Schumacher MA, Dennis IC, Liu CY, et al. NRG4-ErbB4 signaling represses proinflammatory macrophage activity. *Am J Physiol - Gastrointest Liver Physiol*. 2021;320(6):G990-G1001. doi:10.1152/AJPGI.00296.2020

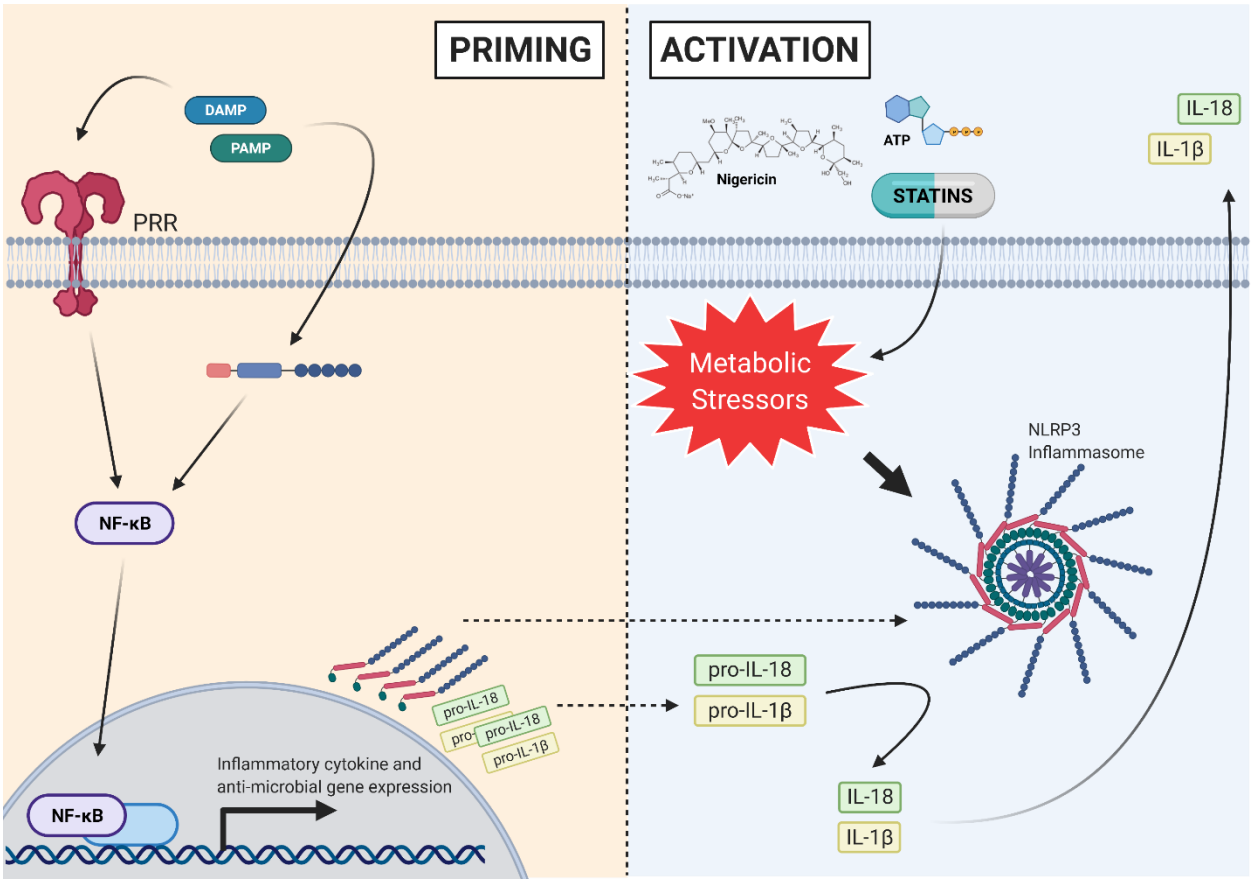

Figure 1: Mechanism of NLRP3 Inflammasome Priming and Activation.

Priming: Pattern- or damage-associated molecular patterns (PAMPs, DAMPs) bind to pattern recognition receptors (PRR) which activates nuclear factor κB (NF-κB). NF-κB subsequently translocate into the nucleus to upregulate inflammatory cytokine and inflammasome component gene expression. Activation: Metabolic stressors like nigericin, high ATP, or xenobiotics like statins, trigger the assembly of inflammasome components into the active NLRP3 inflammasome. Caspase-1-mediated cleavage of pro-IL-1β and pro-IL-18 converts them into their bioactive forms for secretion.

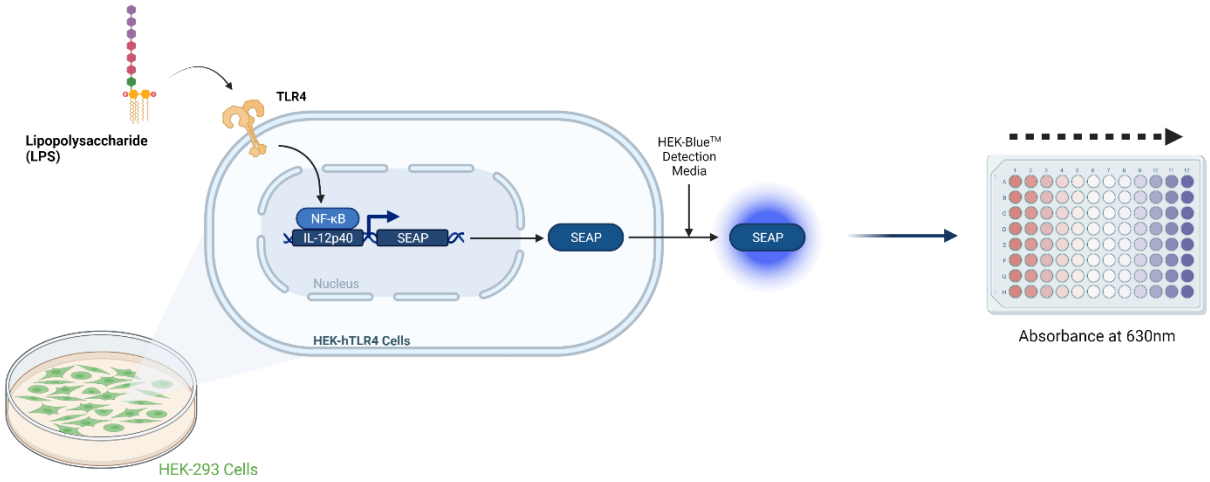

Figure 2: Schematic of NF-κB activation assay using HEK-293T TLR4 reporter system.

Within HEK-293T cells, the secreted embryonic alkaline phosphatase (or SEAP) reporter gene is under the control of a promoter fused to NF-kB binding sites. Stimulation with a TLR4-ligand (like LPS) activates NF-kB, inducing SEAP production which is detected by HEK-Blue™ Detection medium. This detection medium yields a colour change proportional to relative NF-kB activation.

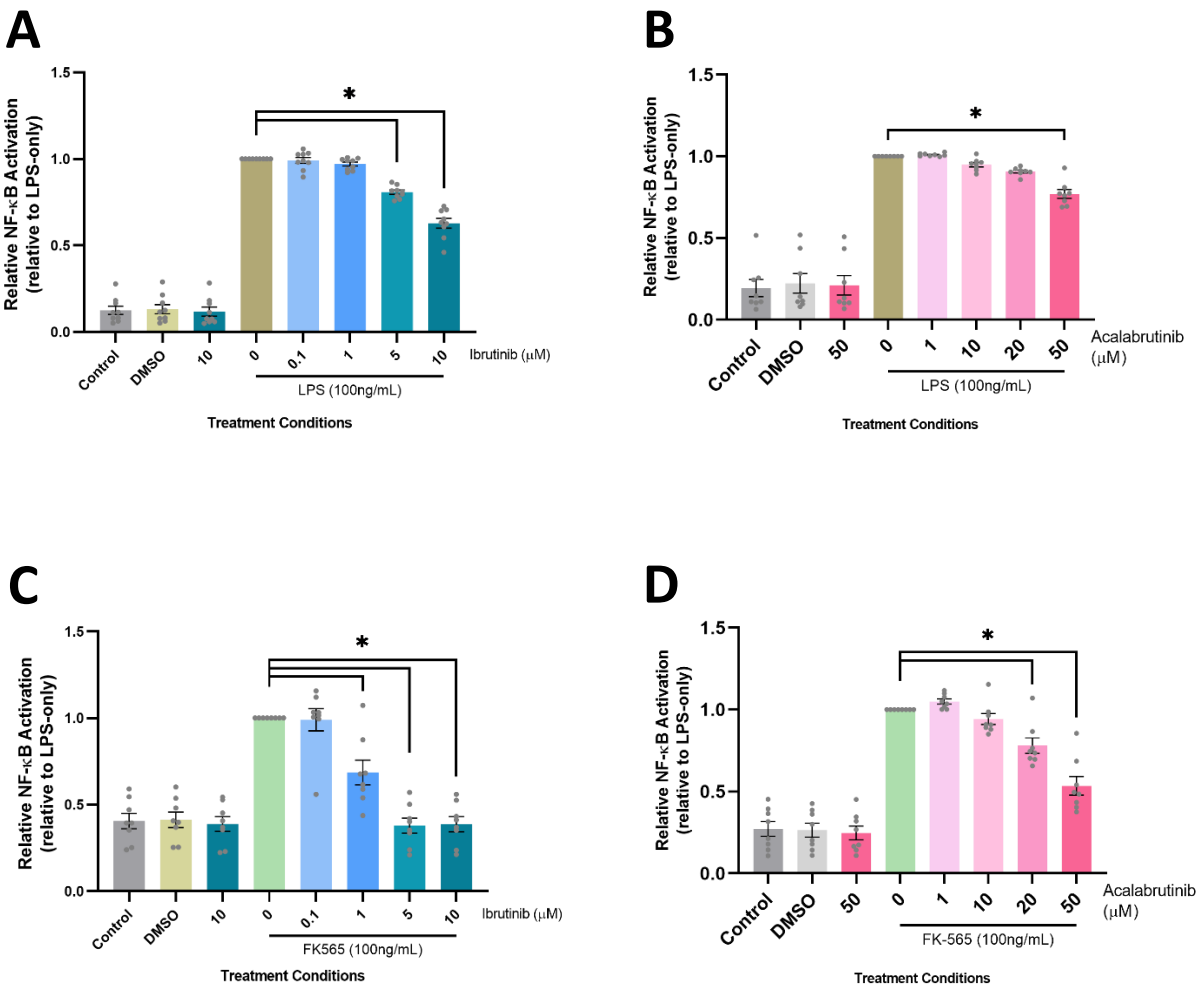

Figure 3: BTK inhibitors lower NF-κB activation by TLR4- and NOD1-ligands. HEK-Blue hTLR4 cells were treated with LPS (100 ng/mL) and Ibrutinib (0.1, 1, 5, 10 μM; panel A) or Acalabrutinib (1, 10, 20, 50 μM; panel B) for 24 hours. HEK-Blue hNOD1 cells were treated with FK-565 (100 ng/mL) and Ibrutinib (0.1, 1, 5, 10 μM; panel C) or Acalabrutinib (1, 10, 20, 50 μM; panel D) for 24 hours. Absorbance of HEK-Blue detection media was quantified by spectrophotometer at 630nm. $P > 0.05$. *Significant difference from corresponding LPS- or FK565-only group. Values are shown as the mean ± SEM. n = 12 for each condition, each n represents a separate experiment on a separate day or cell passage.

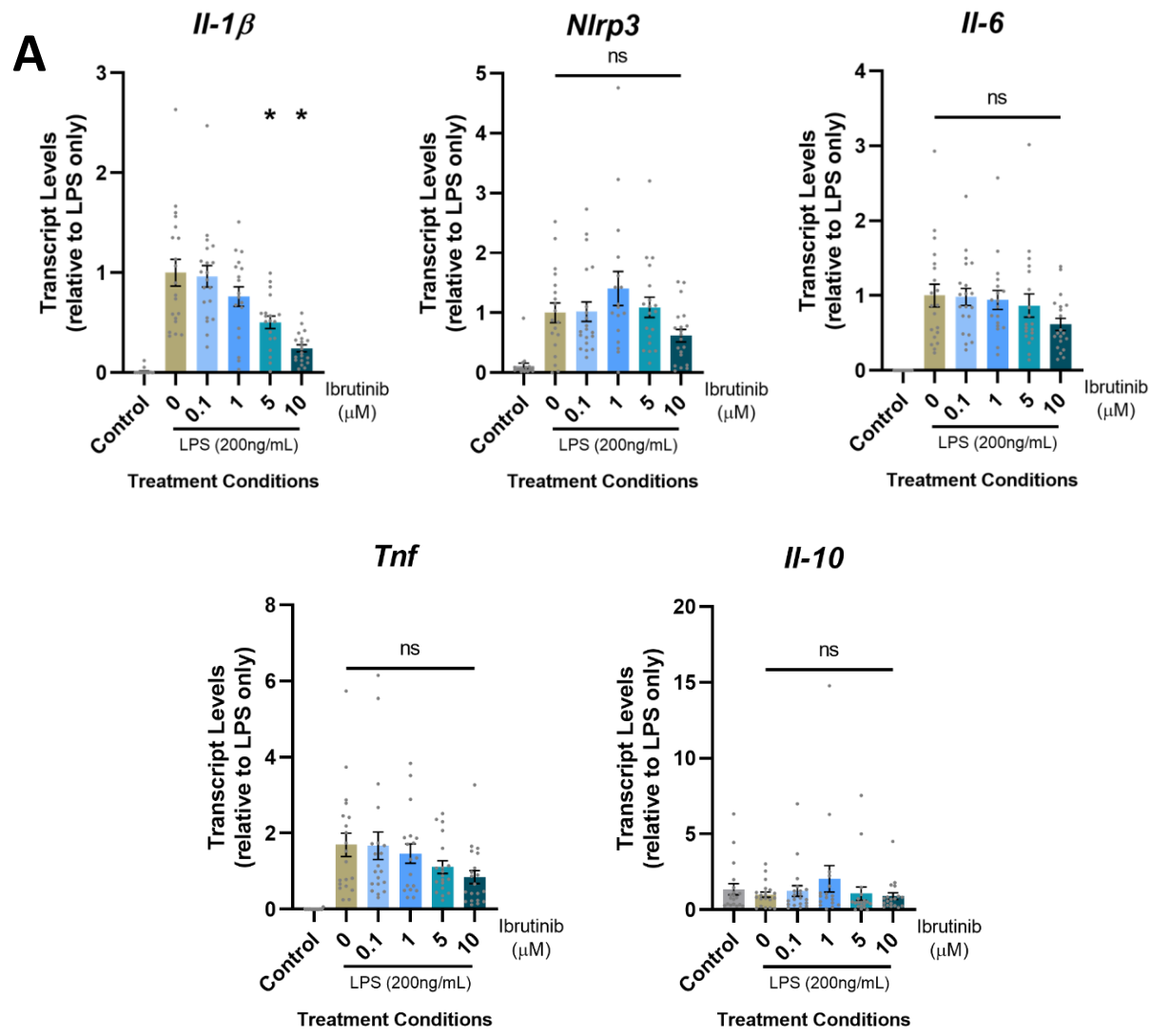
A
Il-1β
Nlrp3
Il-6
Tnf
Il-10
Transcript Levels (relative to LPS only)
ns
* *
Control
0
0.1
1
5
10
Ibrutinib (μM)
LPS (200ng/mL)
Treatment Conditions

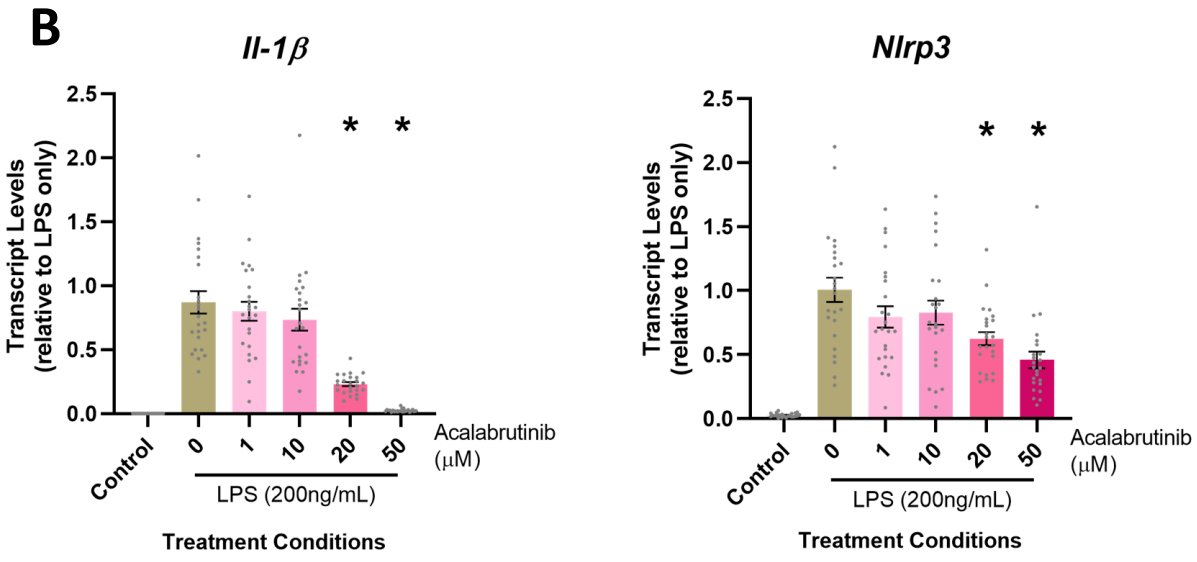
B
Il-1β
Nlrp3
Transcript Levels (relative to LPS only)
* *
Control
0
1
10
20
50
Acalabrutinib (μM)
LPS (200ng/mL)
Treatment Conditions

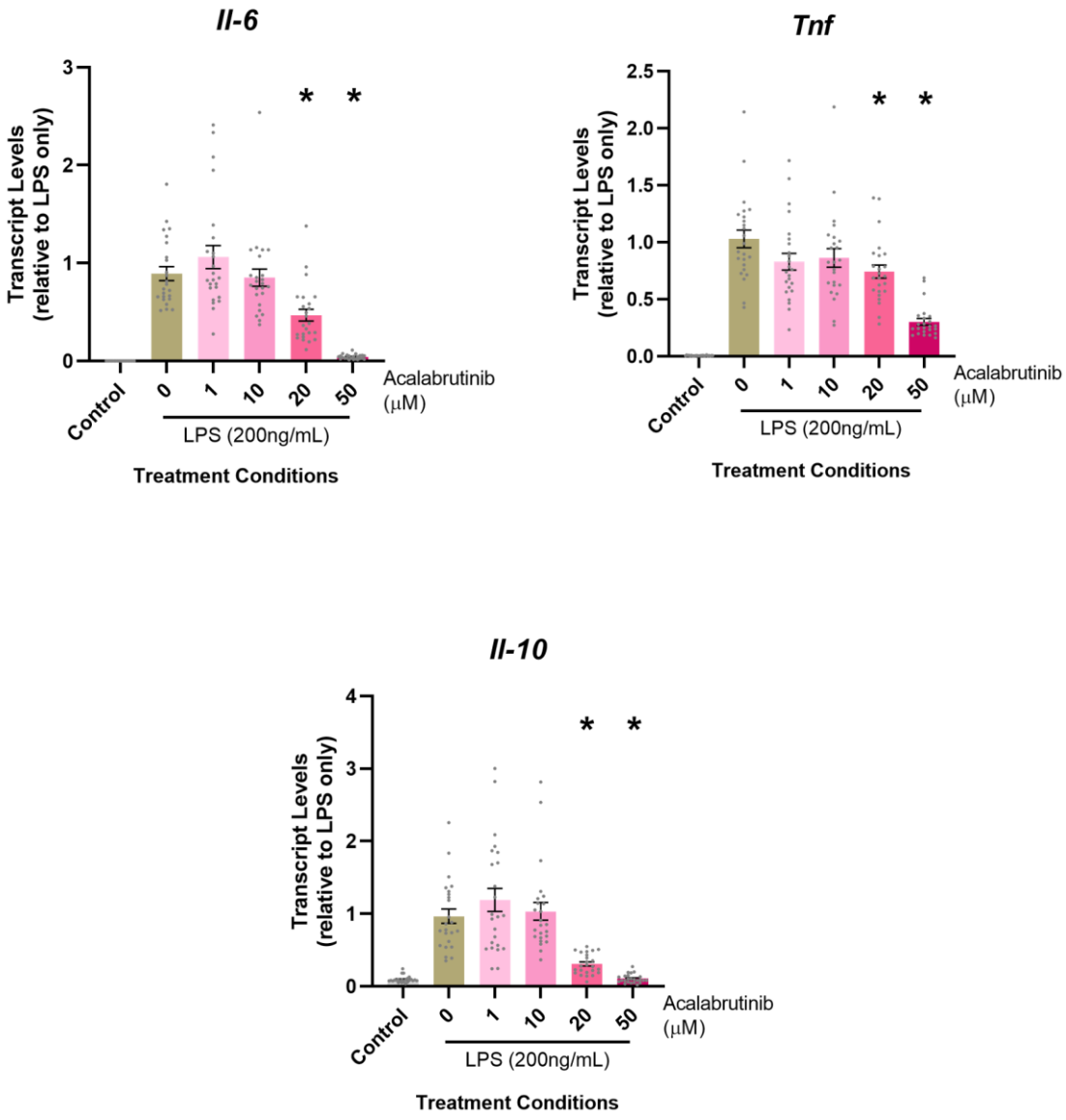

Figure 4: BTK inhibitor treatment mitigates LPS-induced elevation in inflammatory gene expression. BMDMs from WT mice were primed with LPS (200ng/mL, 4 hours) and treated (A) with ibrutinib (0.1, 1, 5, 10 μM, 22 hours) or (B) with acalabrutinib (1, 10, 20, 50 μM, 22 hours). Transcript levels of cytokines were measured by qPCR. $P < 0.05$. *Significant difference from LPS-only condition. Values are shown as the mean ± SEM.

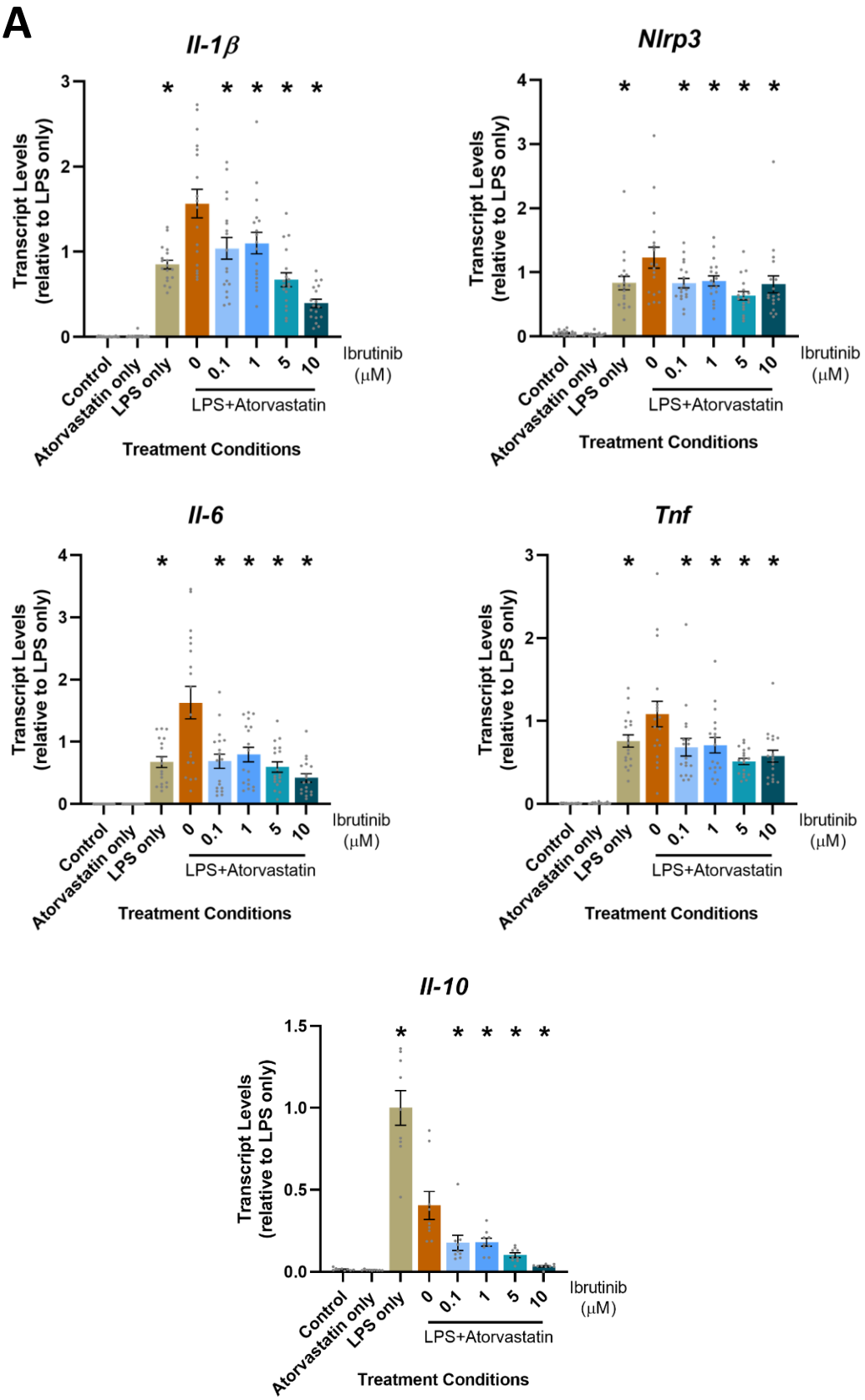
A
Il-1β
Nlrp3
Il-6
Tnf
Il-10
Transcript Levels (relative to LPS only)
Control
Atorvastatin only
LPS only
0
0.1
1
5
10
Ibrutinib (μM)
LPS+Atorvastatin
Treatment Conditions

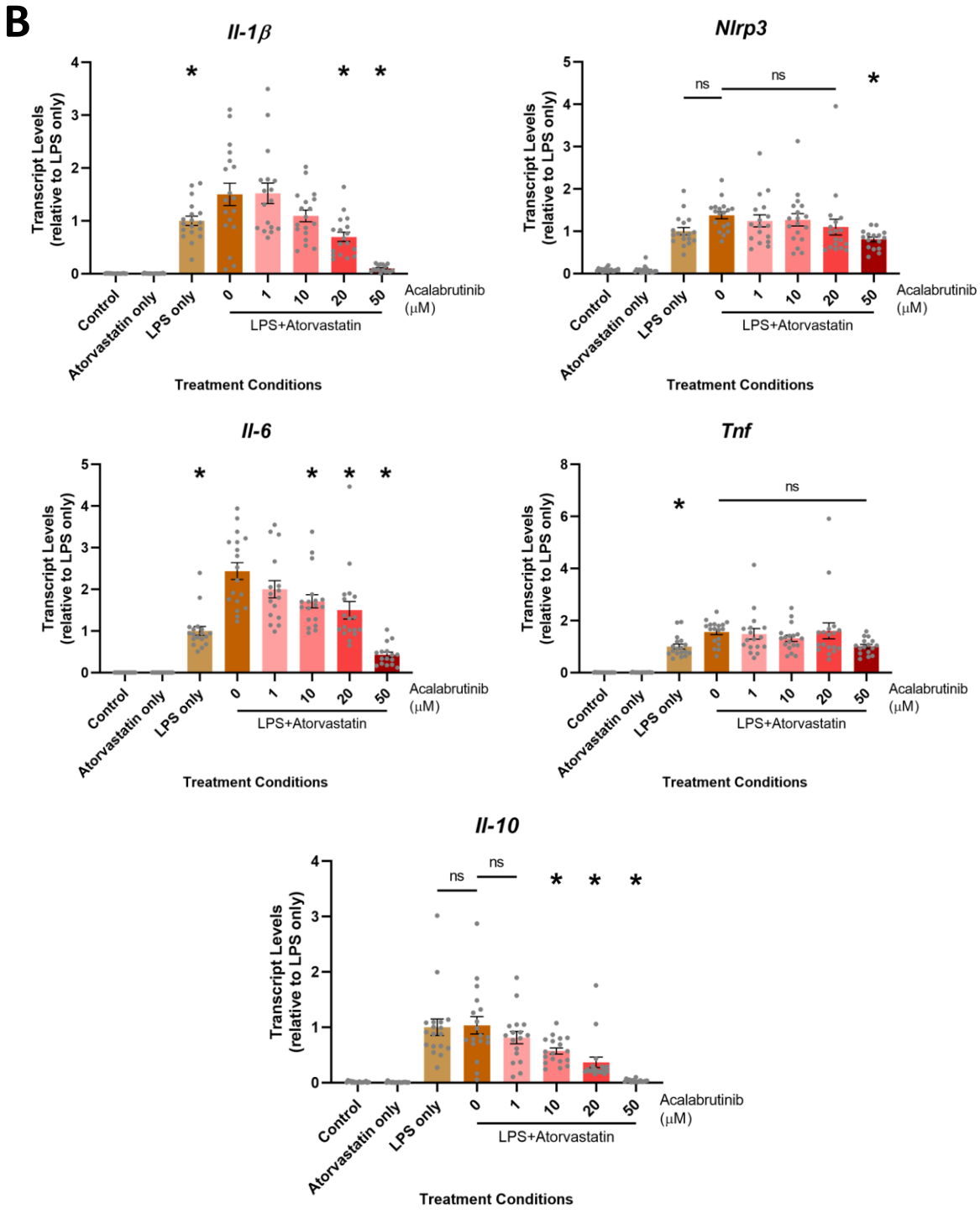

Figure 5: <u>BTK inhibitor treatment reduces LPS-induced elevation in inflammatory gene expression, irrespective of statin exposure.</u> BMDMs from WT C57BL/6J mice were primed with LPS (200ng/mL, 4 hours), and treated with Atorvastatin (1 μM, 22 hours), and either with ibrutinib (0.1, 1, 5, 10 μM, 22 hours) or (B) with acalabrutinib (1, 10, 20, 50 μM, 22 hours). Transcript levels of cytokines were measured by qPCR. $P < 0.05$. *Significant difference from LPS-only condition. Values are shown as the mean ± SEM.

A

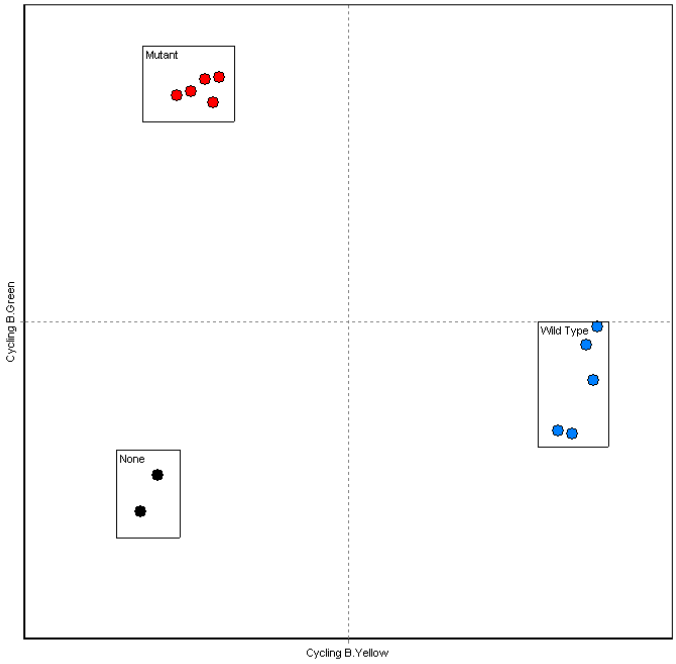

B

Allelic analysis - Cycling B.Green, Cycling B.Yellow				
No.	**Name**	**Genotype**	**Cycling B.Green**	**Cycling B.Yellow**
1	WT	Wildtype	No Reaction	Reaction
2	MUT	Mutant	Reaction	No Reaction
3	NTC		No Reaction	No Reaction
4	Water		No Reaction	No Reaction
5		Wildtype	No Reaction	Reaction
6		Wildtype	No Reaction	Reaction
7		Wildtype	No Reaction	Reaction
8		Wildtype	No Reaction	Reaction
9		Mutant	Reaction	No Reaction
10		Mutant	Reaction	No Reaction
11		Mutant	Reaction	No Reaction
12		Mutant	Reaction	No Reaction

Figure 6: End-point analysis genotyping of CBA/CaJ and CBA/CaHN-Btk^{xid}/J mice strains. Samples were combined with probes specific to sequence of either CBA/CaJ or CBA/CaHN-Btk^{xid}/J strains and ran on a manually inputted temperature profile using the Rotor-Gene Q system. Channel Yellow refers to wild-type specific probe, channel green refers to mutant specific probe. A) Scatter analysis graph is presented distinguishing the individual plots according to their genotypes. B) Result table of allelic discrimination analysis showing genotype and reaction with specific fluorescent probes indicated. All 10 genotype results were consistent with the mice strain of origin and the no-template control (NTC), and water results provided suitable controls, as expected.

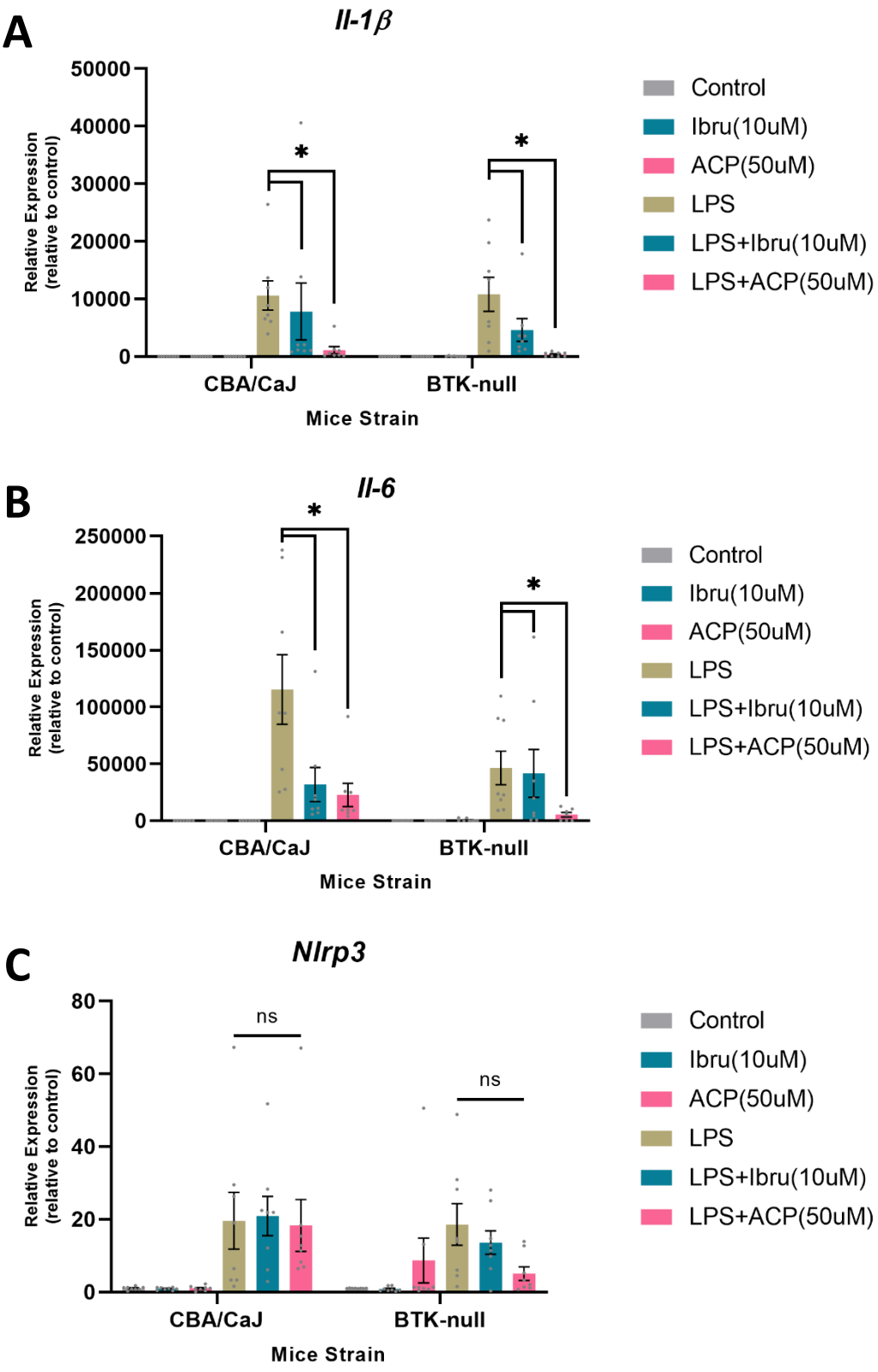
A
Il-1β
Relative Expression (relative to control)
50000
40000
30000
20000
10000
0
*
*
CBA/CaJ
BTK-null
Mice Strain
Control
Ibru(10uM)
ACP(50uM)
LPS
LPS+Ibru(10uM)
LPS+ACP(50uM)
B
Il-6
Relative Expression (relative to control)
250000
200000
150000
100000
50000
0
*
*
CBA/CaJ
BTK-null
Mice Strain
Control
Ibru(10uM)
ACP(50uM)
LPS
LPS+Ibru(10uM)
LPS+ACP(50uM)
C
Nlrp3
Relative Expression (relative to control)
80
60
40
20
0
ns
ns
CBA/CaJ
BTK-null
Mice Strain
Control
Ibru(10uM)
ACP(50uM)
LPS
LPS+Ibru(10uM)
LPS+ACP(50uM)

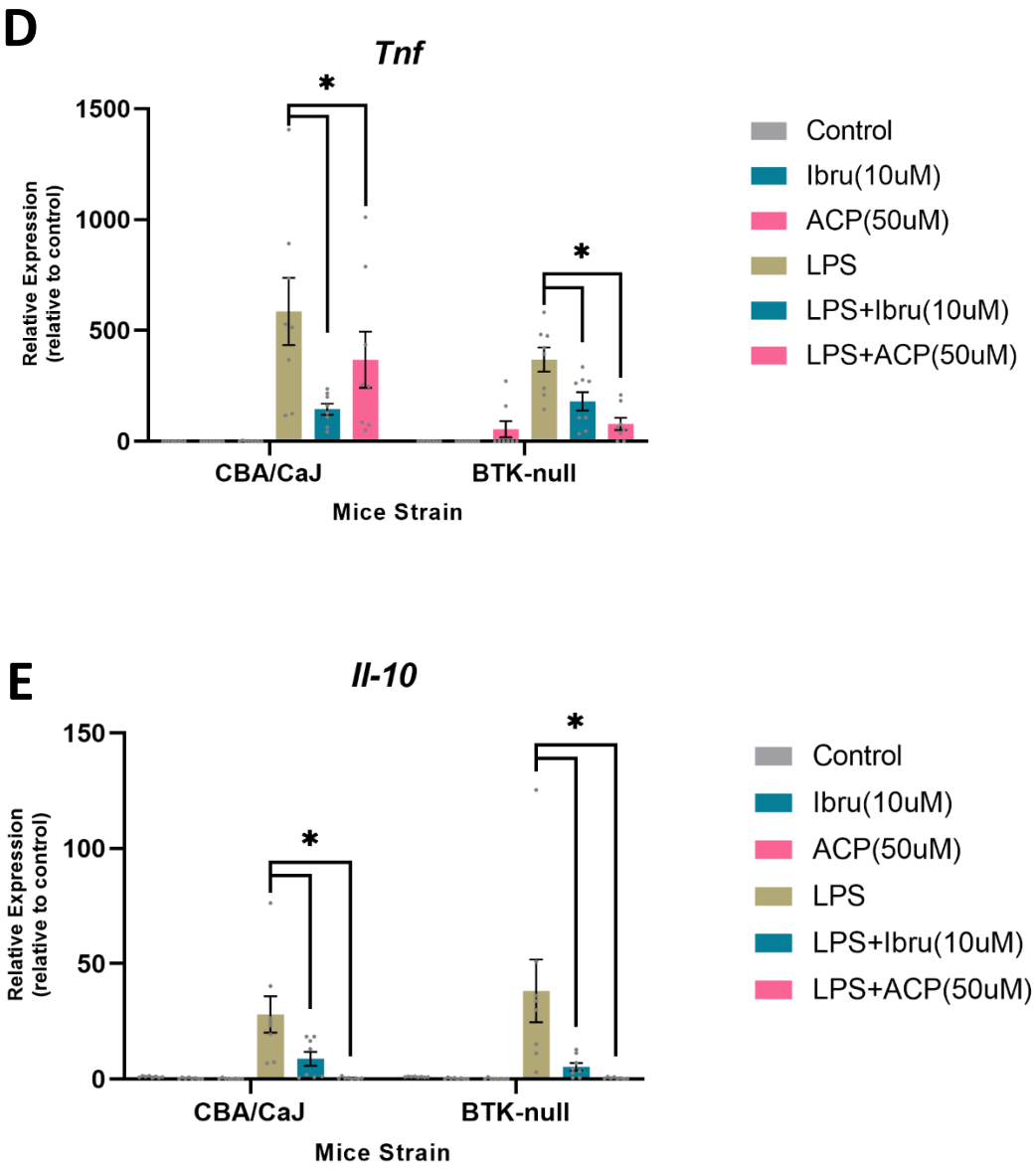

Figure 7: BTK inhibitors do not require BTK to lower inflammatory cytokines in murine macrophages. BMDMs from CBA/CaJ (CBA-WT) and CBA/CaHN-Btk^{xid}/J (BTK-null) were primed with LPS (200 ng/mL, 4 hours), and either Ibrutinib (10 µM, 22 hours) or Acalabrutinib (ACP, 50 µM, 22 hours). Transcript levels of (A) *Il-1β*, (B) *Il-6*, (C) *Nlrp3*, (D) *Tnf*, and (E) *Il-10*, were assessed by quantitative PCR. $P < 0.05$. *Significant difference from corresponding group shown by connecting lines. Values are shown as the mean ± SEM. n = 8-10 for each condition, each n represents an individual treatment well.

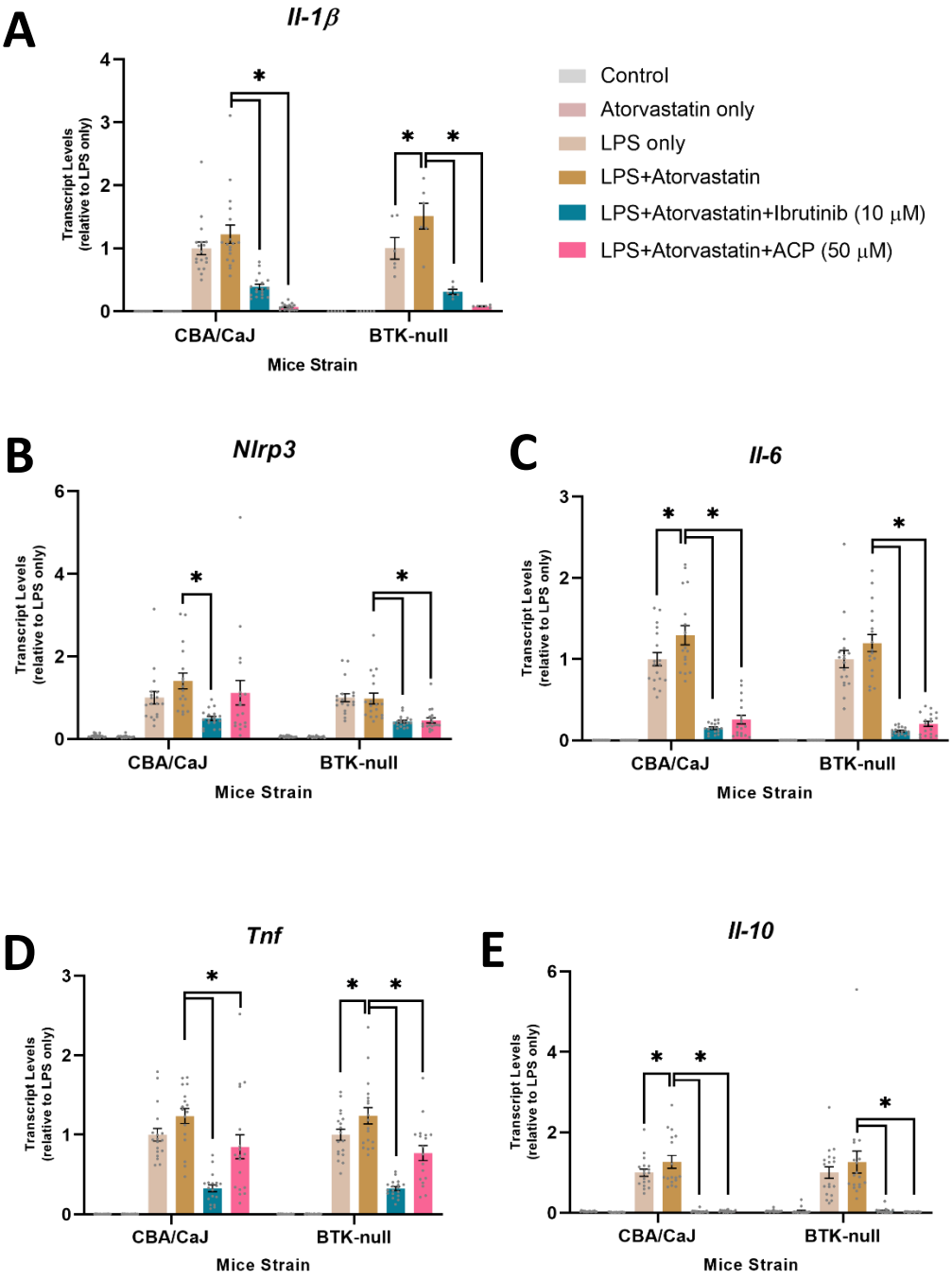

Figure 8: <u>BTK inhibitors do not require BTK to mitigate inflammatory gene expression elevated by inflammasome activator challenge.</u> BMDMs from CBA-WT and BTK-null mice were primed with LPS (200ng/mL, 4 hours), Atorvastatin (1 μM, 22 hours), and treated with ibrutinib (10 μM, 22 hours) or acalabrutinib (ACP, 50 μM, 22 hours). Transcript levels of (A) *Il-1β*, (B) *Nlrp3*, (C) *Il-6*, (D) *Tnf*, and (E) *Il-10* were measured by qPCR. $P < 0.05$. *Significant difference from LPS+Atorvastatin only condition of corresponding strain. Values are shown as the mean ± SEM. n = 18 for each condition, each n represents an individual treatment well.

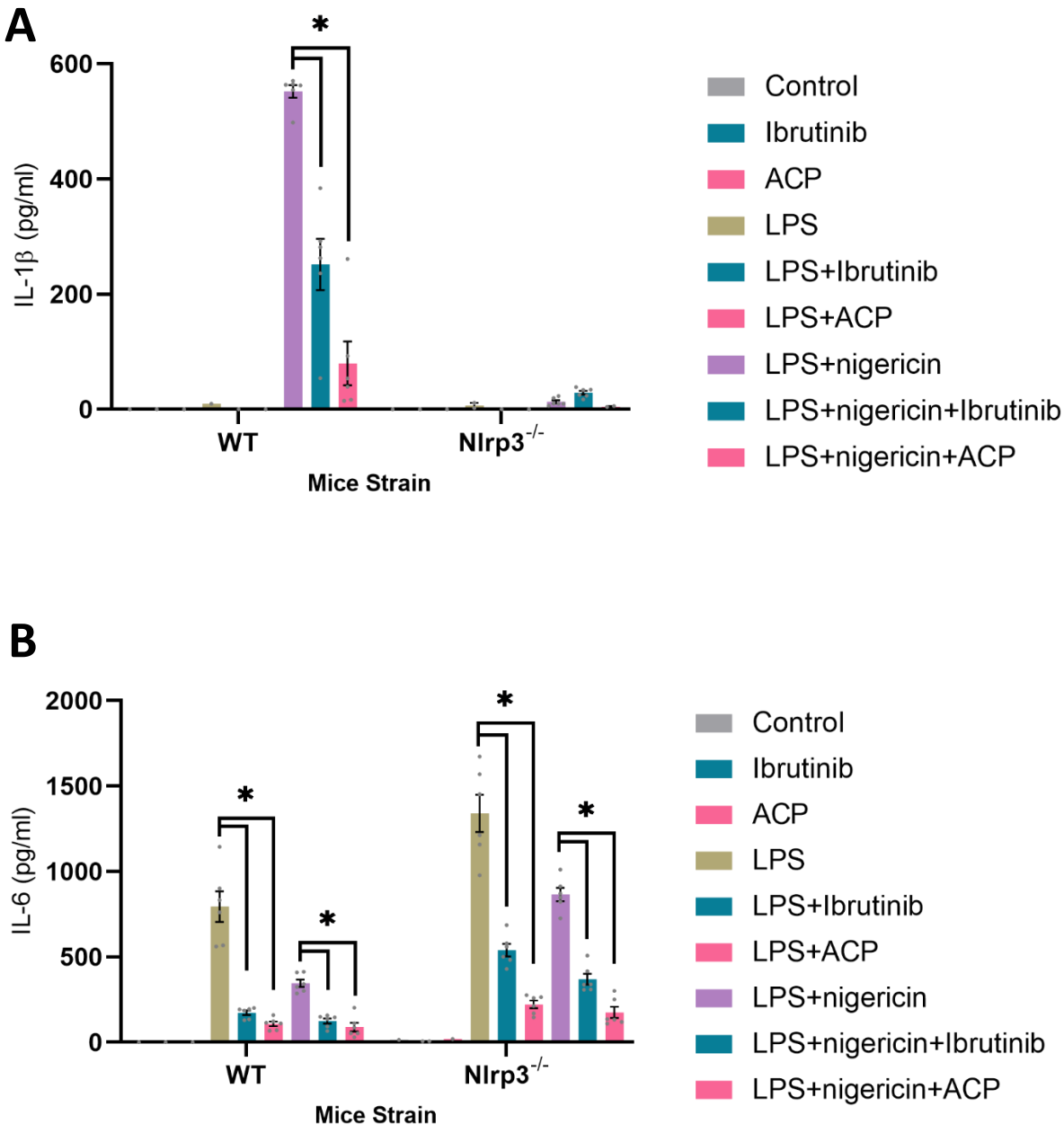

Figure 9: BTK inhibitors lower NLRP3 inflammasome effectors and other cytokines. BMDMs from C57BL/6J or *Nlrp3*$^{-/-}$ mice were primed with LPS (200 ng/mL, 4 hours), treated with nigericin (20 µM, 30 minutes), and either Ibrutinib (10 µM, 22 hours) or Acalabrutinib (ACP, 50 µM, 22 hours). (A) IL-1β, and (B) IL-6 secretion levels were quantified by ELISA. $P < 0.05$. *Significant difference from corresponding group shown by connecting lines. Values are shown as the mean ± SEM. n = 6 for each condition, each n represents an individual treatment well.

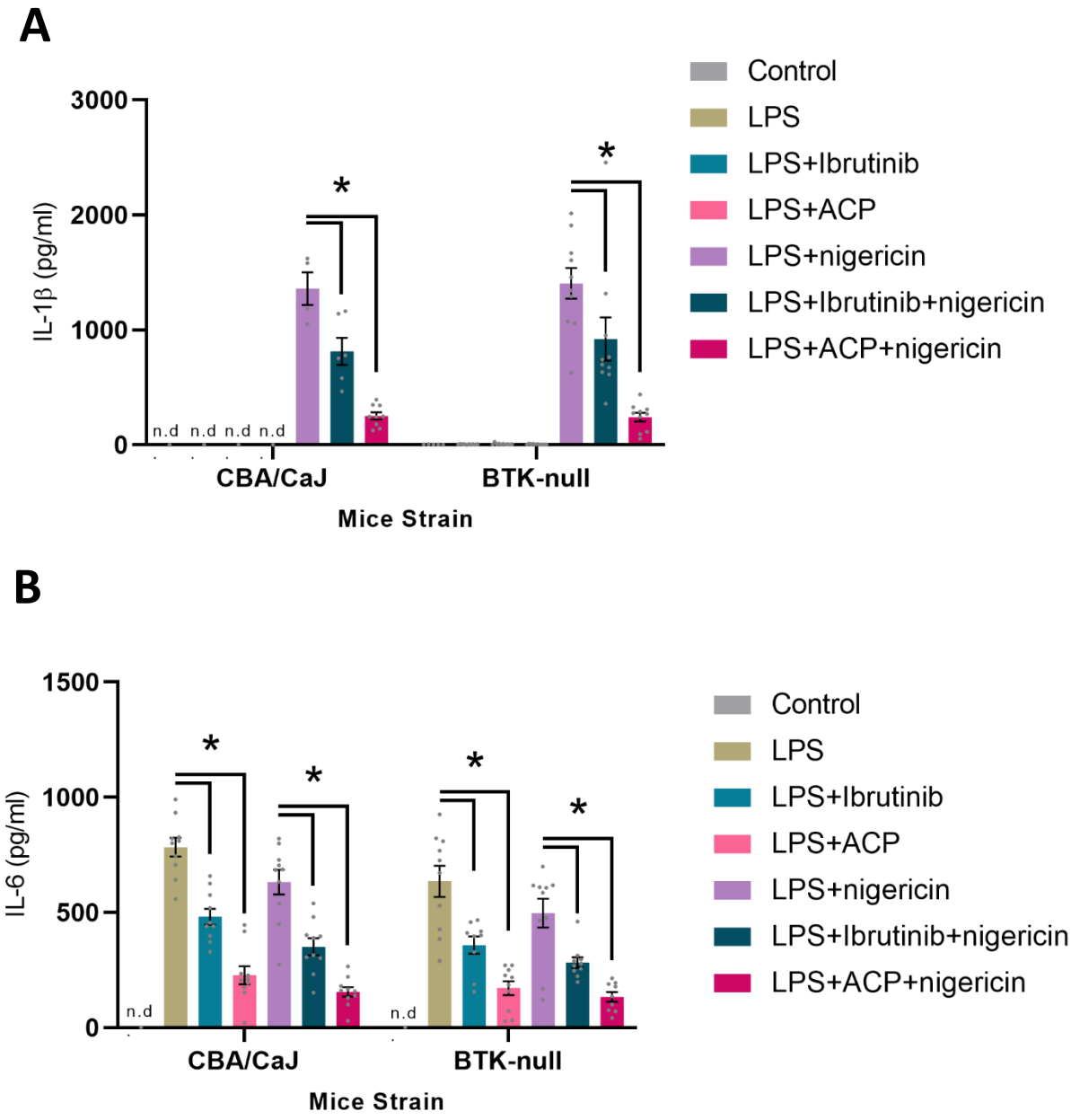

Figure 10: <u>BTK inhibition lowers LPS-induced IL-1β and IL-6 secretions via a BTK-independent mechanism.</u> BMDMs from CBA-WT or BTK-null mice were primed with LPS (200 ng/mL, 4 hours), treated with nigericin (20 µM, 30 minutes), and either Ibrutinib (10 µM, 22 hours) or Acalabrutinib (ACP, 50 µM, 22 hours). Cell-conditioned supernatants from the same samples as those in figure 7 were analyzed for (A) IL-1β, and (B) IL-6 secretion levels by ELISA. $P < 0.05$. *Significant difference from corresponding group shown by connecting lines. Values are shown as the mean ± SEM. n = 8-10 for each condition, each n represents an individual treatment well.

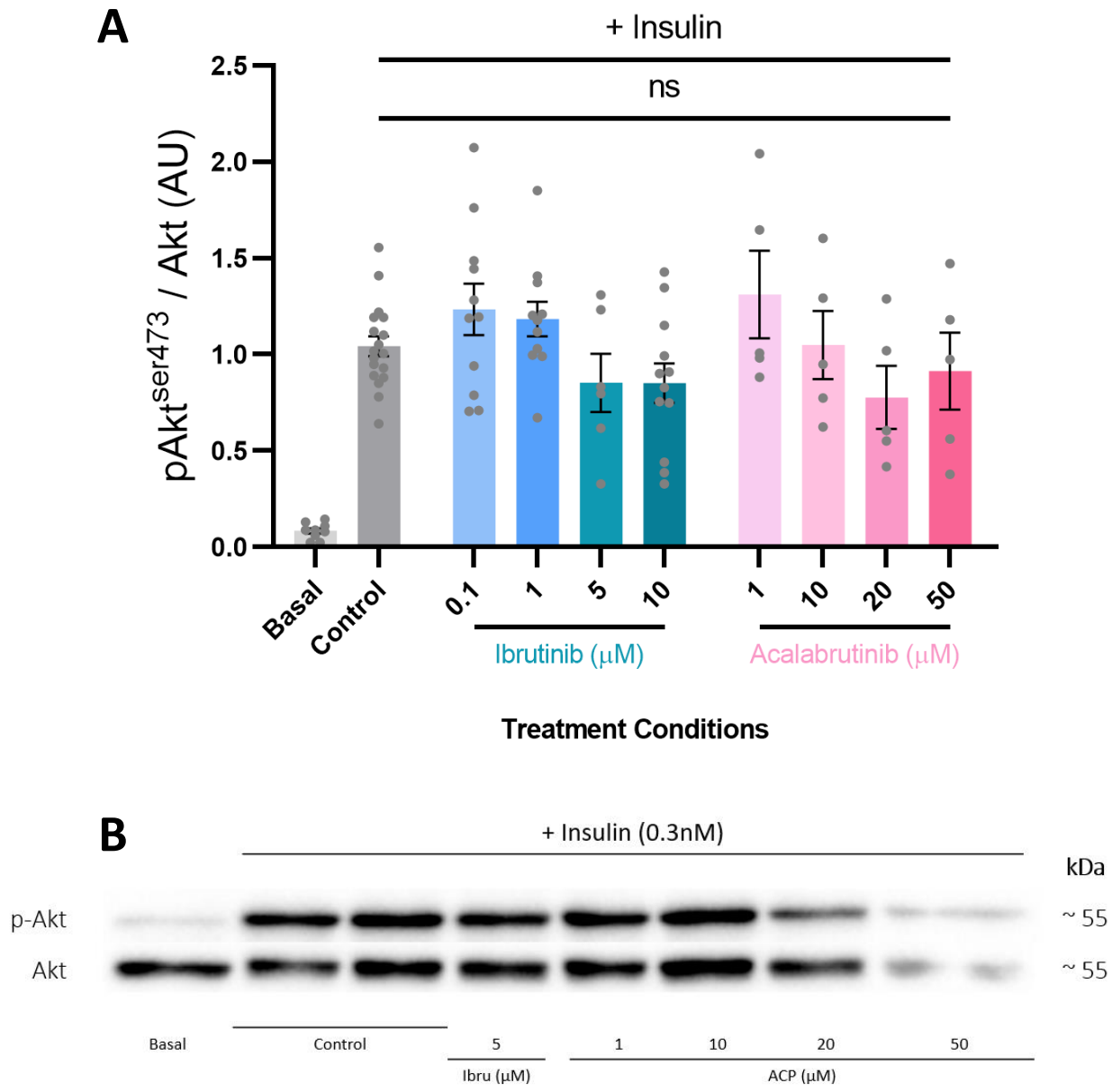

Figure 11: BTK inhibitor treatment alone does not affect insulin signaling in adipose tissue *ex vivo*. (A) Adipose Tissue explants extracted from C57BL/6J mice were treated with Ibrutinib (0.1, 1, 5, 10 µM, 22 hours) or Acalabrutinib (1, 10, 20, 50 µM, 22 hours). All conditions except basal were stimulated with insulin for the last 10 minutes of treatment (0.3 nM). The protein content of these explants was isolated, purified, and quantified by immunoblotting. The quantified band intensities were converted into p-Akt-to-Akt ratios and plotted here. (B) Representative gel for part of the experiment. $P < 0.05$. ns represent no significant difference. Values are shown as the mean ± SEM. n = 12-18, each n represents an individual treatment well.

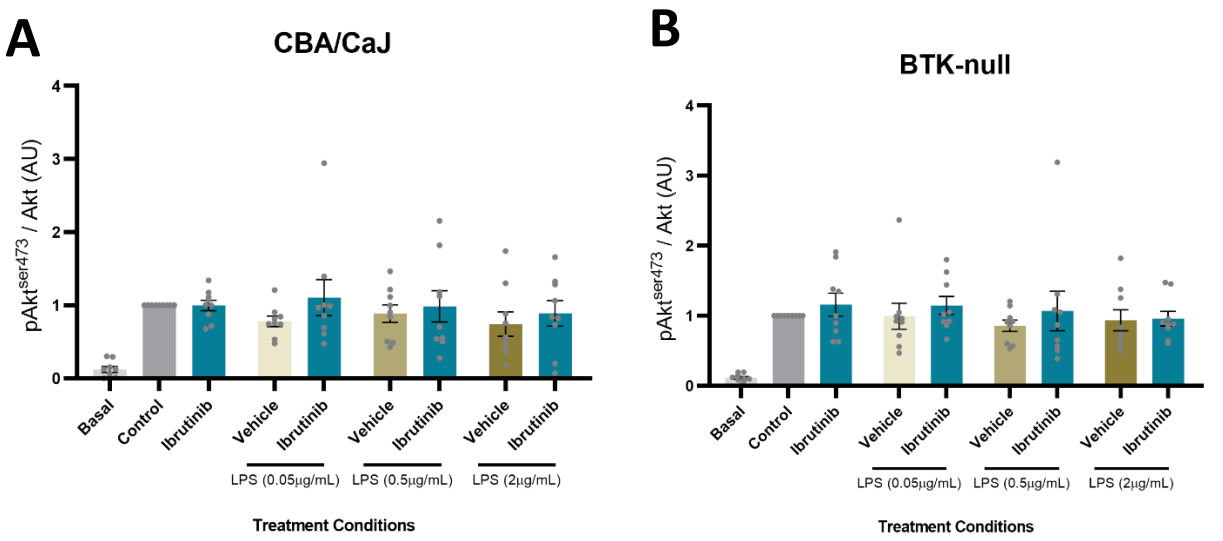
A
CBA/CaJ
pAkt^ser473 / Akt (AU)
Basal
Control
Ibrutinib
Vehicle
Ibrutinib
Vehicle
Ibrutinib
Vehicle
Ibrutinib
LPS (0.05μg/mL)
LPS (0.5μg/mL)
LPS (2μg/mL)
Treatment Conditions
B
BTK-null
pAkt^ser473 / Akt (AU)
Basal
Control
Ibrutinib
Vehicle
Ibrutinib
Vehicle
Ibrutinib
Vehicle
Ibrutinib
LPS (0.05μg/mL)
LPS (0.5μg/mL)
LPS (2μg/mL)
Treatment Conditions

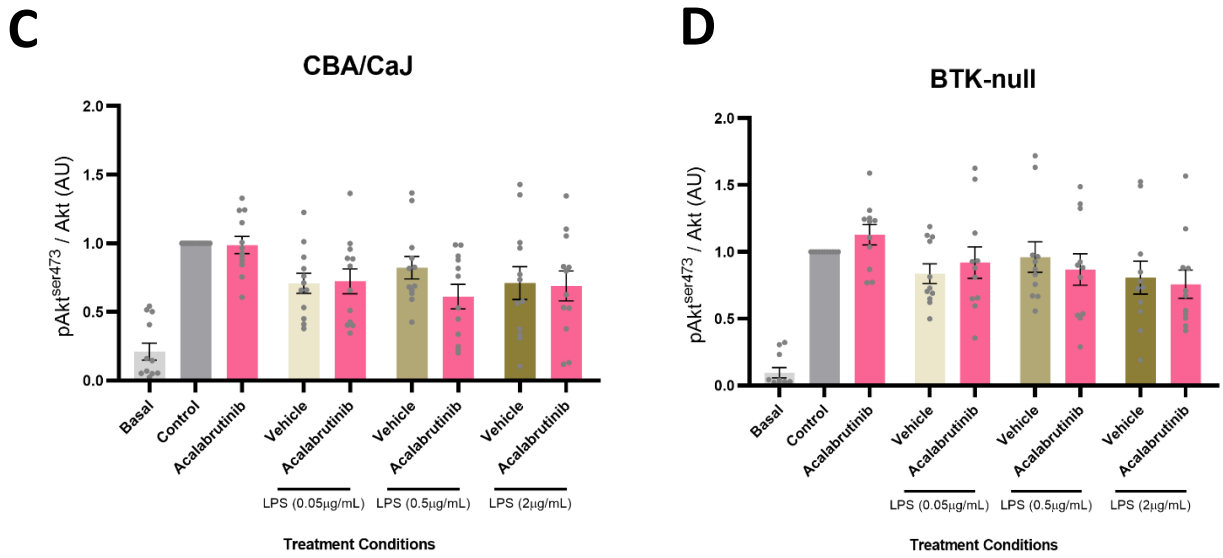
C
CBA/CaJ
pAkt^ser473 / Akt (AU)
Basal
Control
Acalabrutinib
Vehicle
Acalabrutinib
Vehicle
Acalabrutinib
Vehicle
Acalabrutinib
LPS (0.05μg/mL)
LPS (0.5μg/mL)
LPS (2μg/mL)
Treatment Conditions
D
BTK-null
pAkt^ser473 / Akt (AU)
Basal
Control
Acalabrutinib
Vehicle
Acalabrutinib
Vehicle
Acalabrutinib
Vehicle
Acalabrutinib
LPS (0.05μg/mL)
LPS (0.5μg/mL)
LPS (2μg/mL)
Treatment Conditions

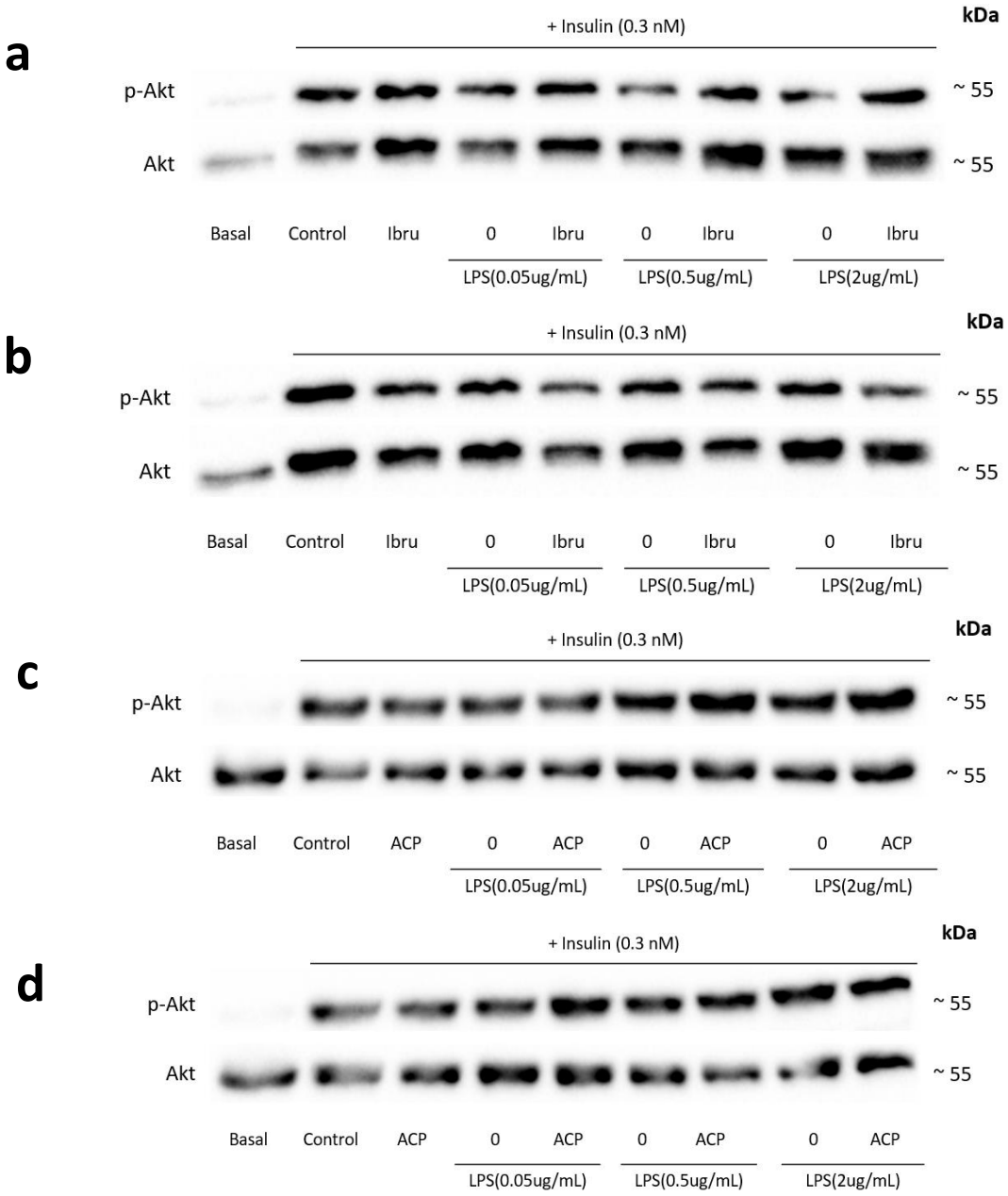

Figure 12: LPS treatment at doses up to 2 µg/mL has no effect on insulin signaling in adipose tissue *ex vivo*. Adipose tissue explants extracted from CBA-WT mice were primed with LPS (0.05, 0.5, 2 µg/mL, 4 hours), and treated with either Ibrutinib (Ibru, 10 µM, 22 hours, panel A) or Acalabrutinib (ACP, 50 µM, 22 hours, panel C). The same experiment is repeated with adipose tissue explants from BTK-null mice, treated with Ibrutinib (panel B), treated with Acalabrutinib (panel D). All conditions except basal were stimulated with insulin for the last 10 minutes of treatment (0.3 nM). The protein content of these explants was isolated, purified, and quantified by immunoblotting. The quantified band intensities were converted into p-Akt-to-Akt ratios and plotted here. (a, b, c, d) Representative gels for panel of the corresponding upper-case letter. $P < 0.05$. ns represent no significant difference. Values are shown as the mean ± SEM. n = 9, each n represents an individual treatment well.

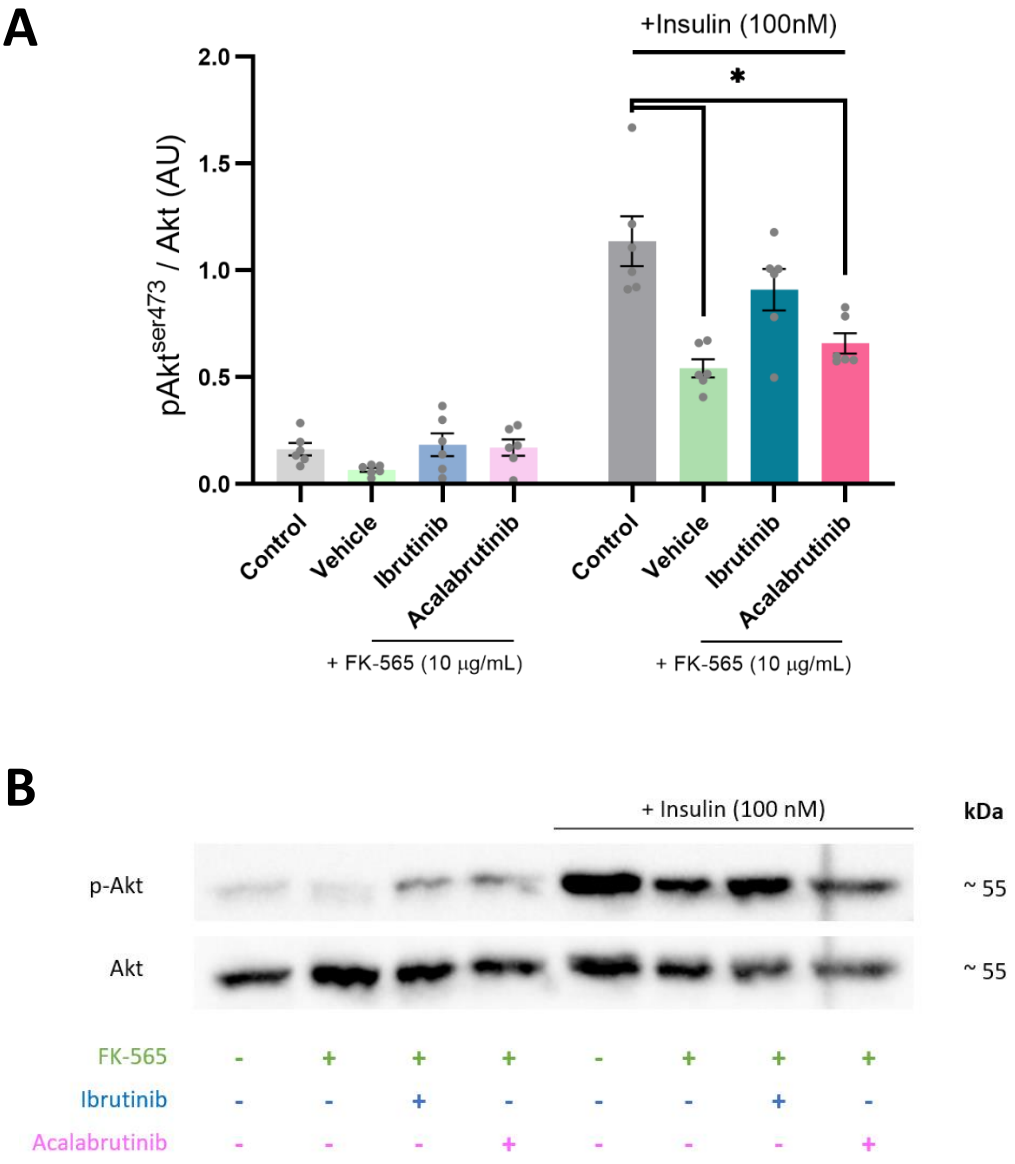

Figure 13: BTK inhibitors attenuate bacterial cell wall-mediated insulin resistance in 3T3-L1 adipocytes. (A) 3T3-L1 adipocytes were pre-incubated with either ibrutinib (10 µM) or acalabrutinib (50 µM) for 1 hour followed by treatment with FK-565 (10 µg/mL) for 48 hours. Insulin stimulated conditions were treated with insulin (100 nM) for the 10 minutes prior to the end of treatment. The protein content of these adipocytes was isolated, purified, and quantified by immunoblotting. The quantified band intensities were converted into p-Akt-to-Akt ratios and plotted here. (B) Representative gel for part of the experiment. $P < 0.05$. * Significant difference compared to insulin-stimulated control condition. Values are shown as the mean ± SEM. n = 6, each n represents an individual treatment well.

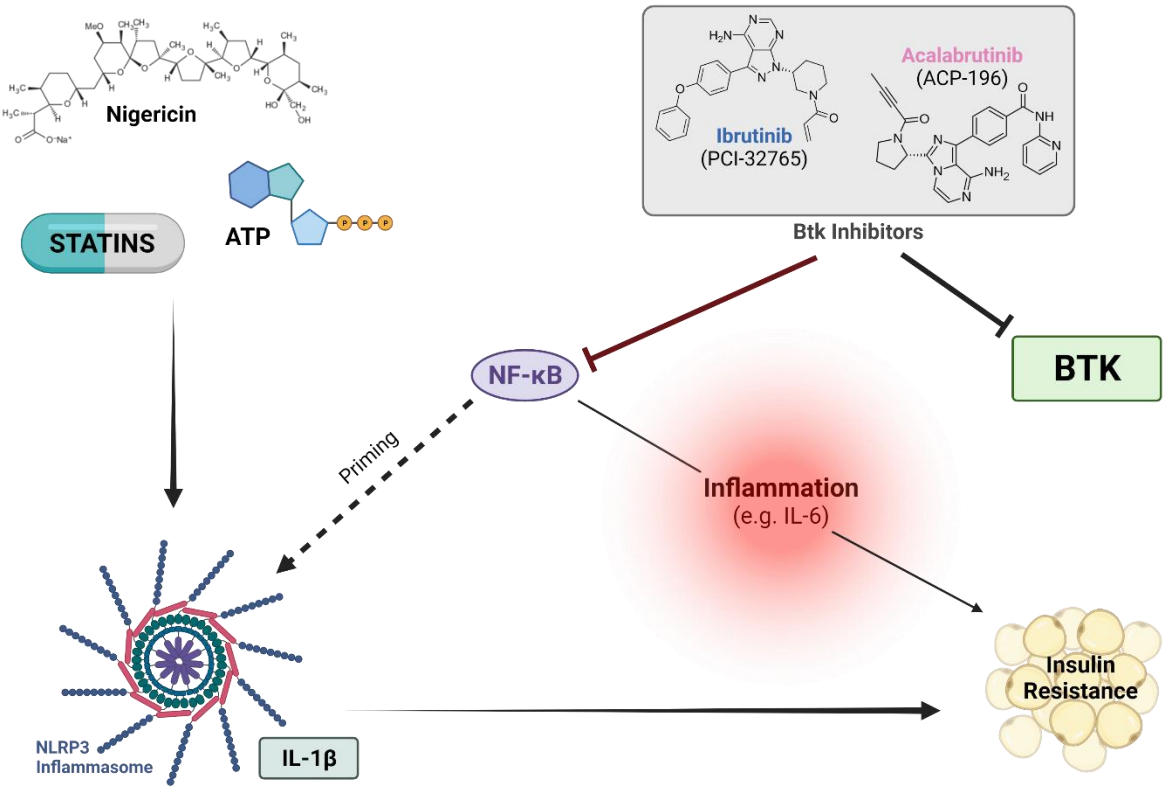

Figure 14: Schematic concluding key findings from the thesis

In addition to a priming signal, metabolic stress signals like nigericin, high ATP, and xenobiotics like statins all can activate the NLRP3 inflammasome. Statins induce adipose tissue insulin resistance via the inflammasome and IL-1β. Throughout this thesis, we demonstrated that ibrutinib and acalabrutinib inhibit NF-κB activation, which consequently lead to lowering of inflammatory gene expression and cytokine secretion. The two BTK inhibitors confer this anti-inflammatory effect independent of BTK. Future directions of this project help bridge the knowledge gap and determine if BTK inhibitors can ameliorate metabolic dysfunction induced by inflammasome activators, like statins.

Table 4: Kinase binding profile of ibrutinib and acalabrutinib by KINOMEscan®[76,77]

Target	Description	Family	Percentage of control	
			Ibrutinib	Acalabrutinib
BTK	Bruton's tyrosine kinase	Tec	0	0.05
ERBB2	Receptor tyrosine-protein kinase erbB-2	EGFR	0	2.1
ERBB4	Receptor tyrosine-protein kinase erbB-4	EGFR	0	4.3
TEC	Tyrosine kinase expressed in hepatocellular carcinoma	Tec	5.7	6.4
LIMK1	LIM domain kinase 1	LISK	30	13
TXK	Tyrosine-protein kinase	Tec	1.4	24
BMX	Bone marrow tyrosine kinase on chromosome X	Tec	14	34
TNNI3K	Serine/threonine-protein kinase TNNI3K	MLK	73	38
BRAF(V600E)	Serine/threonine-protein kinase B-raf	RAF	50	44
KIT(V559D)	Mast/stem cell growth factor receptor Kit	PDGFR	25	53
CSNK2A1	Casein kinase II subunit alpha	CK2	57	54
KIT(V559D, T670I)	Mast/stem cell growth factor receptor Kit	PDGFR	98	55
p38 - δ	Mitogen-activated protein kinase 13	MAPK	-	57
FRK	Tyrosine-protein kinase FRK	Src	14	59
MARK2	Serine/threonine-protein kinase MARK2	CAMKL	100	59
YANK2	Serine/threonine-protein kinase 32B	YANK	77	59
RIPK2	Receptor-interacting serine/threonine-protein kinase 2	RIPK	5	60
BLK	Tyrosine-protein kinase Blk	Src	0.1	61
HCK	Tyrosine-protein kinase HCK	Src	0.6	62
KIT(L576P)	Mast/stem cell growth factor receptor Kit	PDGFR	23	63
BRAF	Serine/threonine-protein kinase B-raf	RAF	53	64
MST2	Serine/threonine-protein kinase 3	STE20	57	65
PDPK1	3-phosphoinositide-dependent protein kinase 1	PDK1	71	67

SRMS	Tyrosine-protein kinase Srms	Src	0	67
SRPK1	SRSF protein kinase 1	SRPK	60	67
EPHB2	Ephrin type-B receptor 1	Eph	100	69
PRKG1	cGMP-dependent protein kinase	PKG	-	70
JAK1(JH2domain)	Tyrosine-protein kinase JAK1	Jak	100	71
RET(M918T)	Proto-oncogene tyrosine-protein kinase receptor Ret	Ret	18	71
ASK1	Apoptosis signal-regulating kinase 1	MAPK	-	73
LOK	Serine/threonine-protein kinase 10	STE20	40	73
NEK9	Serine/threonine-protein kinase Nek9	NEK	88	73
PAK3	Serine/threonine-protein kinase PAK 3	STE20	39	73
STK33	Serine/threonine-protein kinase 33	STK33	80	73
CDK7	Cyclin-dependent kinase 7	CDK	86	74
EGFR	Epidermal growth factor receptor	EGFR	1.8	75
ACVRL1	Serine/threonine-protein kinase receptor R3	STKR	100	76
EPHA1	Ephrin type-A receptor 1	Eph	61	76
MELK	Maternal embryonic leucine zipper kinase	CAMKL	75	76
PFTAIRE2	Cyclin-dependent kinase 15	CDK	-	76
FGFR3(G697C)	Fibroblast growth factor receptor 3	FGFR	28	77
MERTK	Tyrosine-protein kinase Mer	Axl	90	77
PKAC - α	cAMP-dependent protein kinase catalytic subunit alpha	PKA	80	77
RAF1	RAF proto-oncogene serine/threonine-protein kinase	RAF	70	77
CSNK1G1	Casein kinase I isoform gamma-1	CK1	-	78
PAK2	Serine/threonine-protein kinase PAK 2	STE20	92	78
SRC	Proto-oncogene tyrosine-protein kinase Src	Src	4	78

BRK	Protein-tyrosine kinase 6	Src	-	79
PIM2	Serine/threonine-protein kinase pim-2	PIM	89	79
DAPK2	Death-associated protein kinase 2	DAPK	92	80
NEK7	Serine/threonine-protein kinase Nek7	NEK	94	80
PLK4	Serine/threonine-protein kinase PLK4	PLK	44	80
RIOK2	Serine/threonine-protein kinase RIO2	RIO	95	80
JAK2(JH1domain)	Tyrosine-protein kinase JAK2	Jak	77	81
CDK2	Cyclin-dependent kinase 2	CDK	100	82
CSNK1G2	Casein kinase I isoform gamma 2	CK1	-	82
LYN	Tyrosine-protein kinase Lyn	Src	11	82
MARK3	MAP/microtubule affinity-regulating kinase 3	CAMKL	60	82
MEK2	Dual specificity mitogen-activated protein kinase kinase 2	MAPK	-	82
TNIK	TRAF2 and NCK-interacting protein kinase	STE20	100	82
KIT(D816V)	Mast/stem cell growth factor receptor Kit	PDGFR	77	83
LZK	Mitogen-activated protein kinase kinase kinase 13	MLK	-	83
TESK1	Dual specificity testis-specific protein kinase 1	LISK	86	83
YES	Tyrosine-protein kinase Yes	Src	2	83
AMPK-α2	5'-AMP-activated protein kinase catalytic subunit alpha-2	CAMKL	100	84

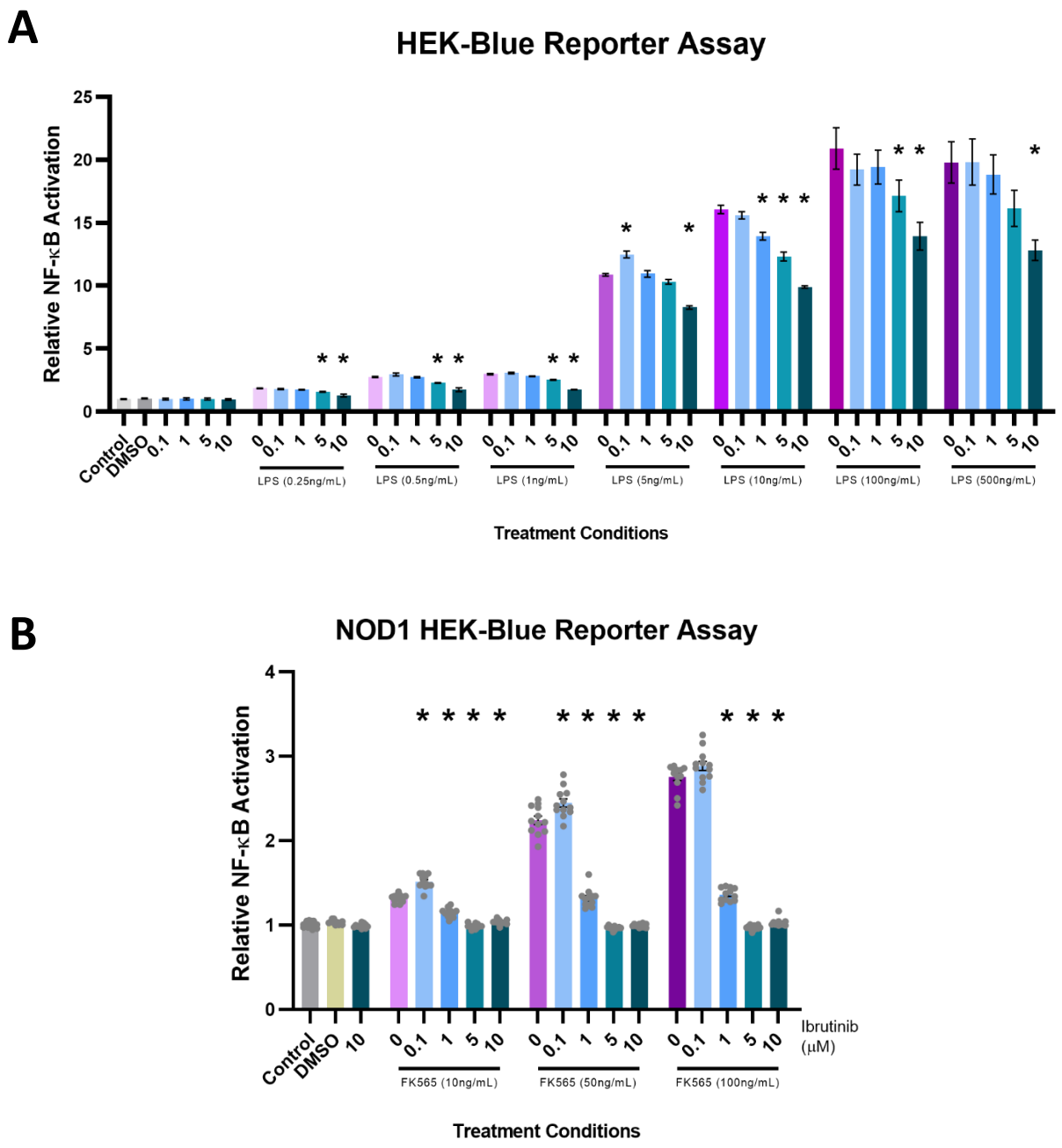

Supplementary Figure 1: Dose response of NF-κB activation induced by TLR4- and NOD1-ligands. (A) HEK-Blue hTLR4 cells were treated with LPS (0.25-500 ng/mL) and Ibrutinib (0.1, 1, 5, 10 μM) for 24 hours. (B) HEK-Blue hNOD1 cells were treated with FK-565 (10-100 ng/mL) and Ibrutinib (0.1, 1, 5, 10 μM) for 24 hours. Absorbance of HEK-Blue detection media was quantified by spectrophotometer at 630nm. $P > 0.05$. *Significant difference from corresponding LPS- or FK565-only group. Values are shown as the mean ± SEM. n = 12 for each condition, each n represents a separate experiment on a separate day or cell passage.